Phase Behavior Modeling for Carbon Dioxide/Brine Mixtures

by

Ziting Sun

A thesis submitted in partial fulfillment of the requirements for the degree of

Master of Science

in

Petroleum Engineering

Department of Civil and Environmental Engineering

University of Alberta

ABSTRACT

Accurately predicting CO_2 solubility in saline aquifers is very important for CO_2 capture and storage. A reliable and accurate thermodynamic model is needed to accurately predict the phase behavior of the CO_2+brine systems over a wide range of temperature, pressure, and molality. This study aims at developing a cubic-equation-of-state-based thermodynamic model that can accurately describe the phase behavior of the CO_2+brine systems. Peng-Robinson equation of state (PR EOS) (Peng & Robinson, 1976) and the Huron-Vidal (HV) mixing rule (Huron and Vidal, 1979) are utilized to model the phase equilibria of CO_2+brine systems containing salt species including NaCl, KCl, $CaCl_2$, and $MgCl_2$. Binary interaction parameters as functions of temperature and salt molality are established for specific CO_2+single-salt+H_2O systems. The model is extended to account for the effects of different salt species on CO_2 solubility in aqueous phase solutions, which can cover the typical geological conditions (273-550K, 0-800 bar, 0-6 mol/kg).

We employ the PR EOS together with the proposed BIP strategy in the HV mixing rule to reproduce the mutual solubility of CO_2 and H_2O in vapor-liquid equilibria (VLE). The collected experimental data are used to determine the optimal BIP model. The validation of the model calculations against the available experimental data indicates that the average absolute percentage error (*%AAD*) in reproducing the CO_2 concentration in the mixed-salt brine is 12.63%. Compared to the calculation results provided by the state-of-the-art models in the literature (Søreide & Whitson, 1992; Sun et al., 2021), the PR EOS together with the proposed BIP strategies in the HV mixing rule can more accurately predict the VLE of CO_2+brine systems over large ranges of temperature, pressure, and molality.

DEDICATION

This dissertation is dedicated to my dearest parents, Mr. Liangwei Sun and Mrs. Xuemei Wei.

ACKNOWLEDGMENTS

I would like to thank my supervisor, Dr. Huazhou (Andy) Li, for his continuous guidance and encouragement during my master program at the University of Alberta. He not only guides me on how to conduct research, but also helps me form a rigorous academic attitude. I also want to thank my examination committee chair, Dr. Bipro Dhar, and the examination committee members, Dr. Carlos Lange and Dr. Juliana Leung, for their critical and valuable comments.

I am grateful for the unconditional love and support from my parents during my studies at the University of Alberta. I would also like to thank my friend Jose Leonardo Guevara Urdaneta; thank you for always being there. I would also like to thank my colleagues (Jialin Shi, Shiyu Yin, and Zixuan Cui) in Dr. Li's research group for their technical suggestions on my thesis work.

TABLE OF CONTENTS

LIST OF TABLES

LIST OF FIGURES

CHAPTER 1 INTRODUCTION

1.1 Research Background

CO_2 emission due to the combustion of fossil fuels is becoming a major concern of global warming and climate change. It is imperative to develop promising technologies that can significantly reduce CO_2 concentration in the atmosphere. Carbon capture, utilization and storage (CCUS) is considered as one of the key technologies.

CO_2 injection into gas and oil reservoirs is one of the typical CCUS technologies. More specifically, CO_2 can be injected into oil reservoirs to enhance oil recovery or gas reservoirs to enhance gas recovery (Abba et al., 2019). During the recovery process, part of the injected CO_2 can be stored in the oil and gas reservoirs. Upon the end of the projects, the produced CO_2 will be injected into the depleted reservoirs to get securely stored there.

CO_2 injection in underground aquifer formations is another promising geological storage technology due to its large storage potential (Bachu et al., 2007; Xiao et al., 2016; Sminchak et al., 2017; Ding et al., 2018). In this context, four key processes can guarantee the permanent immobilization of CO_2: structural trapping, residual gas trapping, solubility trapping, and mineral trapping (Chamwudhiprecha & Blunt, 2011). The solubility trapping mechanism refers to the trapping of CO_2 due to the dissolution of CO_2 in the brine. Therefore, the prediction of CO_2 solubility plays an important role in the reliable estimation of CO_2 storage capacity in saline aquifers. Since aquifer water is seldom pure and usually contains varying amounts of different dissolved salts, the presence of salts can significantly alter the CO_2 solubility in saline aquifers.

Many efforts have been made to apply cubic equation of state (CEOS) models to model the phase behavior of gas/brine mixtures. However, these models still suffer from one limitation, i.e., they cannot be applied to CO_2+mixed-salt+H_2O systems. Therefore, it is highly necessary to further improve the current CEOS modeling framework such that the CEOS models can be applicable to CO_2+mixed-salt+H_2O systems.

1.2 Literature Review of Predicting VLE/LLE in CO_2/Brine Mixture

1.2.1 Methods for Predicting VLE/LLE of Gas/Water Binaries

The existing methods for gas solubility predictions can be divided into two categories: thermodynamic models based on EOS models and empirical correlations. The former method consists of well-known equations that relate pressure, volume, temperature, and composition of a fluid system, e.g., PR EOS (Peng & Robinson, 1976) and SRK EOS (Soave, 1972). The latter method establishes empirical correlations that are regressed on measured phase behavior data.

1.2.2 Thermodynamic Models for Predicting VLE/LLE of CO_2/Brine Binaries

Aquifer water is seldom pure and usually contains varying amounts of different dissolved salts, among which NaCl, KCl, $CaCl_2$, and $MgCl_2$ are the four most seen salts. The presence of salts can significantly alter the CO_2 solubility in the formation water. Since Na^+ and Cl^- are the main species found in the salts of most geological formations, ranging from 10,000-300,000 ppm (Haas, 1976), the NaCl solution is hence the most used system to represent the formation brines (Koschel et al., 2006). The concentration of NaCl in formation brines can range from 10,000 to 300,000 ppm (Haas, 1976).

CEOSs are widely used to predict the volumetric and phase behavior of pure compounds and mixtures by satisfying the condition of chemical equilibrium. Since van der Waals first attempted

to develop a simple empirical EOS for real gas, it has been modified to different expressions. Two of the most popular CEOSs in petroleum engineering applications are the Soave-Redlich-Kwong (SRK) EOS (Soave, 1972) and the Peng-Robinson (PR) EOS (Peng & Robinson, 1976). However, the conventional EOSs have certain deficiencies in modeling the phase equilibria of CO_2/brine mixtures. These deficiencies include they tend to less accurate in predicting water content in the gas phase, and they don't take the impact of different salt types into account. Many efforts have been made to improve the accuracy of thermodynamic models in predicting the phase equilibria of CO_2/brine mixtures by modifying EOSs and its binary interaction parameters (BIPs) in different mixing rules. These efforts are reviewed below.

The thermodynamic modeling methods that can be applied to predict the phase behavior of CO_2 /brine mixtures can be categorized as either symmetric approach (*f-f*) (Trusler, 2017) or asymmetric approach (*g-f*) (Zhao & Lvov, 2016). The symmetric approach uses the same EOS for the liquid-liquid phase equilibria (LLE) and/or vapor-liquid phase equilibria (VLE). Since the disadvantage of the asymmetric approach is that it may result in a thermodynamic inconsistency near the critical region (Zhao & Lvov, 2016), this work is based on the *f-f* method where the thermodynamic model is based on the equality of fugacity of each component throughout all the phases.

Since the traditional CEOSs are intended primarily for hydrocarbon mixtures, several attempts have been made to extend the application area of CEOSs to gas-water and gas-brine mixtures, such as modifying alpha-function, BIP or mixing rules for specific gas-liquid pairs. Søreide & Whitson (1992) modified the traditional PR EOS to predict the solubility of gases and hydrocarbons in pure H_2O system and aqueous NaCl system by developing a specific alpha-term which is a function of NaCl molality and the reduced temperature of pure water. Besides, two different sets of BIPs were

used for the aqueous and non-aqueous phases, with the aqueous phase BIP related to NaCl molality. Unfortunately, as discussed above, using two sets of BIPs can lead to thermodynamic inconsistency issues near the critical region (Zhao & Lvov, 2015). Also, the Søreide & Whitson (1992) model is only dedicated to the CO_2+NaCl+H_2O systems, it may not be accurate in predicting the solubility of CO_2 in brines with other salt species (such as KCl, $CaCl_2$, and $MgCl_2$).

Kiepe et al. (2002) extended the G^E-EOS hybrid model to model CO_2 solubility in NaCl and KCl solutions. Their predicted results are in good agreement with the experimental data, but further measurements need to be carried out in order to fill existing gaps in the PSRK parameter matrix. Bermejo et al. (2005) proposed a thermodynamic model for CO_2+Na_2SO_4+H_2O systems with Anderko-Pitzer EOS (Anderko & Pitzer, 1993), which takes a fully ion-paired molecular basis for the salt into consideration. Their model is specially developed for water-salt systems at high temperatures and pressures, yielding average deviations of 3.73% and 4.64% in reproducing the total pressures of the CO_2+H_2O system and CO_2+H_2O+Na_2SO_4 system, respectively. However, the extrapolated results from the Anderko-Pitzer EOS are not accurate. They pointed out that it is probably because Anderko-Pitzer EOS is very sensitive to the value of the EOS parameters, making it necessary to adjust the EOS parameters at different temperatures and salt concentrations.

Some other models can be categorized as the *g-f* models. More recently, Duan & Sun (2003) proposed a model for calculating CO_2 solubility in H_2O and aqueous NaCl solutions, which applies to a wide temperature-pressure-molality range (0-2000 bar, 273-533 K, 0-4.3 mol/kg). However, the model developed by Duan & Sun (2003) relies on a fifth-order virial EOS (Duan et al., 1992), which cannot be efficiently implemented in numerical flow simulations. Another drawback of Duan's model is that it is not intended to calculate water content in the gas phase. Diamond & Akinfiev (2003) proposed a model that was suitable for CO_2+NaCl+H_2O system below 100°C and

100 MPa. However, the model can only roughly estimate the composition of the gas phase. Later, Springer et al. (2012) developed a model for predicting CO_2 solubility in chloride salt systems based on the mixed solvent electrolyte model and SRK EOS.

1.3 Problem Statement

The aforementioned models, developed for CO_2+H_2O systems and CO_2+salt+H_2O systems, have their own strengths and weaknesses. Most of the models developed so far are dedicated to CO_2+NaCl+H_2O systems. The literature review indicates that the main drawback of these models is they cannot be extended to CO_2+mixed-salt+H_2O systems. Furthermore, some of them appear to be less accurate because they are developed based on limited experimental data.

1.4 Research Objectives

The objective of this work is to develop a model that can accurately predict the CO_2 solubility in brine mixtures and overcome the above limitations. The model consists of a modified version of PR EOS with the Huron-Vidal mixing rule. More specifically, we aim to develop an empirical equation to estimate the BIPs in the Huron-Vidal mixing rule as functions of temperature and molality. This empirical equation will be established by matching the measured CO_2 solubility in four brine systems (NaCl, KCl, $CaCl_2$, and $MgCl_2$), as well as measured CO_2 solubility in pure water system. The experimental data are retrieved from the literature. We lastly want to examine the performance of the developed thermodynamic model by applying it to CO_2+mixed-salt+H_2O systems. The accuracy provided by the established model is to be compared against the most used literature models (Søreide & Whitson, 1992; Sun et al., 2021).

1.5 Thesis Structure

This thesis is comprised of four chapters as follows:

(1) **Chapter 1** introduces the research background, literature review, problem statement, research objectives, and thesis structure.

(2) **Chapter 2** introduces the methodology employed in this study, including all the fundamental equations and models, data collection, objective functions and error indices, Huron-Vidal mixing rule and its BIP strategies. This chapter also presents the principal mechanisms of the non-linear regression algorithm as well as the two-phase flash calculations.

(3) **Chapter 3** demonstrates the performance of the optimal BIP strategy in reproducing VLE/LLE data for the specific CO_2+single-salt+H_2O systems, and CO_2+mixed-salt+H_2O systems. Comprehensive comparisons of experimental VLE/LLE data for the above mixtures against calculated ones from different models are also presented in this chapter.

(4) **Chapter 4** summarizes the conclusions achieved in this study as well as the recommendations for future work.

References

Abba, M.K., Abbas, A.J., Nasr, G.G., Al-Otaibi, A., Burby, M., Saidu, B., & Suleiman, S.M. (2019). Solubility trapping as a potential secondary mechanism for CO_2 sequestration during enhanced gas recovery by CO_2 injection in conventional natural gas reservoirs: an experimental approach. *Journal of Natural Gas Science and Engineering*, 71, 103002.

Anderko, A., & Pitzer, K.S. (1993). Equation-of-state representation of phase equilibria and volumetric properties of the system NaCl-H_2O above 573 K. *Geochimica Et Cosmochimica Acta*, 57(8), 1657-1680.

Bachu, S., Bonijoly, D., Bradshaw, J., Burruss, R., Holloway, S., Christensen, N.P., & Mathiassen, O.M. (2007). CO_2 storage capacity estimation: Methodology and gaps. *International Journal of Greenhouse Gas Control*, 1(4), 430-443.

Bermejo, M.D., Martín, A., Florusse, L.J., Peters, C.J., & Cocero, M.J. (2005). The influence of Na_2SO_4 on the CO_2 solubility in water at high pressure. *Fluid Phase Equilibria*, 238(2), 220-228.

Chamwudhiprecha, N., & Blunt, M.J. (2011). CO_2 storage potential in the North Sea. *In International Petroleum Technology Conference*. *OnePetro*.

Diamond, L.W., & Akinfie, N.N. (2003). Solubility of CO_2 in water from -1.5 to 100°C and from 0.1 to 100 MPa: Evaluation of literature data and thermodynamic modelling. *Fluid Phase Equilibria*, 208(1-2), 265-290.

Ding, S., Xi, Y., Jiang, H., & Liu, G. (2018). CO_2 storage capacity estimation in oil reservoirs by solubility and mineral trapping. *Applied Geochemistry*, 89, 121-128.

Duan, Z., Møller, N., & Weare, J.H. (1992). An equation of state for the CH_4-CO_2-H_2O system: II. Mixtures from 50 to 1000°C and 0 to 1000 bar. *Geochimica Et Cosmochimica Acta*, 56(7), 2619-2631.

Duan, Z., & Sun, R. (2003). An improved model calculating CO_2 solubility in pure water and aqueous NaCl solutions from 273 to 533 K and from 0 to 2000 bar. *Chemical Geology*, 1(1-2), 257-271.

Haas, J.L. (1976). Physical properties of the coexisting phases and thermochemical properties of the H_2O component in boiling NaCl solutions. *Geological Survey Bulletin*, 1421, 24-30.

Kiepe, J., Horstmann, S., Fischer, K., & Gmehling, J. (2002). Experimental determination and prediction of gas solubility data for CO_2+H_2O mixtures containing NaCl or KCl at temperatures between 313 and 393 K and pressures up to 10 MPa. *Industrial and Engineering Chemistry Research*, 41(17), 4393-4398.

Koschel, D., Coxam, J.Y., Rodier, L., & Majer, V. (2006). Enthalpy and solubility data of CO_2 in water and NaCl(aq) at conditions of interest for geological sequestration. *Fluid Phase Equilibria*, 247(1-2), 107-120.

Peng, D., & Robinson, D.B. (1976). A new two-constant equation of state. *Industrial And Engineering Chemistry Research*, 15(1), 59-64.

Sminchak, J.R., Babarinde, O., & Gupta, N. (2017). Integrated analysis of geomechanical factors for geologic CO_2 Storage in the midwestern United States. *Energy Procedia*, 114, 3267-3272.

Soave, G. (1972). Equilibrium constants from a modified Redlich-Kwong equation of state. *Chemical Engineering Science*, 27(6), 1197-1203.

Søreide, I., & Whitson, C.H. (1992). Peng-Robinson predictions for hydrocarbons, CO_2, N_2, and H_2S with pure water and NaCl brine. *Fluid Phase Equilibria*, 77(1), 217-240.

Springer, R.D., Wang, Z., Anderko, A., Wang, P., & Felmy, A.R. (2012). A thermodynamic model for predicting mineral reactivity in supercritical carbon dioxide: I. Phase behavior of carbon dioxide-water-chloride salt systems across the H_2O-rich to the CO_2-rich regions. *Chemical Geology*, 322, 151-171.

Sun, X., Wang, Z., Li, H., He, H., & Sun, B. (2021). A simple model for the prediction of mutual solubility in CO_2-brine system at geological conditions. *Desalination*, 504(1-2), 114972.

Trusler, J.P.M. (2017). Thermophysical properties and phase behavior of fluids for application in carbon capture and storage processes. *Annual Review of Chemical and Biomolecular Engineering*, 8(1), 381402.

Xiao, T., McPherson, B., Pan, F., Esser, R., Jia, W., Bordelon, A., & Bacon, D. (2016). Potential chemical impacts of CO_2 leakage on underground source of drinking water assessed by quantitative risk analysis. *International Journal of Greenhouse Gas Control*, 50, 305-316.

Zhao, H., Fedkin, M.V., Dilmore, R.M., & Lvov, S.N. (2015). Carbon dioxide solubility in aqueous solutions of sodium chloride at geological conditions: Experimental results at 323.15, 373.15, and 423.15 K and 150 bar and modeling up to 573.15 K and 2000 bar. *Geochimica Et Cosmochimica Acta*, 149, 165-189.

CHAPTER 2 METHODOLOGY

2.1 PR EOS Model

The PR EOS has the following form (Peng and Robinson, 1976):

$$p = \frac{RT}{v-b} - \frac{a(T)}{v(v+b)+b(v-b)} \tag{1}$$

$$a(T) = \frac{0.45724\alpha(T)R^2T_c^2}{P_c^2} \tag{2}$$

$$b = \frac{0.07780RT_c}{P_c} \tag{3}$$

$$\alpha(T) = (1 + m(1 - (\frac{T}{Tc})^{0.5}))^2 \tag{4}$$

$$m = 0.37464 + 1.54226\omega - 0.2699\omega^2 \tag{5}$$

where p is the pressure, T is the absolute temperature, R is the universal gas constant, v is the molar volume, a and b are the EOS parameters, T_c is the critical temperature, P_c is the critical pressure, $\alpha(T_r, \omega)$ is the alpha function, which is the function of the reduced temperature and acentric factor, and ω is the acentric factor.

2.2 Huron-Vidal Mixing Rule and its BIPs

The choice of mixing rule and its BIPs is crucial for extending the PR EOS to mixtures. The classical quadratic mixing rule (Wong & Sandler, 1992) combined with special BIPs for the EOS is applicable to mixtures composed of non-polar contents. This is assuming that any phase of the system is homogeneous. However, due to the difference in the polarity of gas and water molecules, this assumption is not valid for mixtures containing polar and non-polar components, making the

classical mixing rule insufficient in representing the phase equilibria when water exists in addition to gas phases.

A few non-classical mixing rules have been proposed by modifying the α-term in the conventional EOS constant a (Wong & Sandler, 1992). The non-classical mixing rules normally adopt the G_{∞}^{E} model derived from a modified non-random two-liquid (NRTL) model (Henri, 1968). Most of those methods have the drawback that the mixing rule cannot be reduced to the classical mixing rule in the absence of non-polar components.

Huron & Vidal (1979) proposed a new polynomial mixing rule in EOS for representing vapour-liquid equilibria of strongly non-ideal mixtures by considering the excess Gibbs energy for predicting the VLE of a highly polar system. This improved the accuracy of mutual solubility predictions for mixtures containing non-polar components. Niels & Michelsen (2007) pointed out that a very useful feature of the Huron-Vidal mixing rule is that it is capable of handling mixtures of hydrocarbons and polar compounds alike, allowing for a proper description of the behavior of the polar compounds while maintaining the classical model for the hydrocarbon compounds. That means, for the mixtures with no polar compounds, the HV mixing rule can be reduced to the classical mixing rule. Note that this is a great advantage of the Huron-Vidal mixing rule. Sørensen et al. (2002) pointed out that the HV mixing rule is recommended for CO_2+NaCl+H_2O, CO_2+KCl+H_2O, CO_2+$CaCl_2$+H_2O systems. That is because the CO_2 solubility in the aqueous phase obtained with the Huron-Vidal mixing rule is more accurate than that obtained with the classical mixing rule.

For the above reasons, in this study, the Huron-Vidal mixing rule is used as the primary mixing rule. The Huron-Vidal mixing rule can be expressed as (Huron & Vidal, 1979):

$$a_m = b_m \left[\sum_{i=1}^{n} z_i \frac{a_i}{b_i} - \frac{G_\infty^E}{C^*} \right] \tag{6}$$

$$b_m = \sum_{i=1}^{n} \sum_{j=1}^{n} z_i \, z_j \frac{(b_i + b_j)}{2} \tag{7}$$

where n is the number of components in the system, z_i is the mole fraction of the i_{th} component, i and j are component indicates, $C^*$is 0.62323 for PR-EOS, and G_∞^E is the excess Gibbs energy at infinite pressure. In this case, G_∞^E can be calculated using a modified NRTL mixing rule (Renon and Praunitz, 1968):

$$G_\infty^E = \sum_{i=1}^{n} z_i \frac{\sum_{j=1}^{n} G_{ji} C_{ji} z_j}{\sum_{k=1}^{n} G_{ki} z_k} \tag{8}$$

where

$$G_{ji} = b_j \, exp\left(-c_{ji} \frac{C_{ji}}{RT}\right) \qquad (Gij = 0 \; when \; i = j; \; c_{ji} = 0 \; when \; i = j) \tag{9}$$

$$C_{ji} = g_{ji} - g_{ii} \tag{10}$$

$$g_{ii} = -C^* \frac{a_i}{b_i} \tag{11}$$

$$g_{ij} = -2 \frac{\sqrt{b_i b_j}}{b_i + b_j} \sqrt{g_{ii} g_{jj}} \left(1 - k_{ij}\right) \qquad (k_{ij} = 0 \; when \; i = j) \tag{12}$$

where α_{ij} is the non-randomness parameter, g_{ii} and g_{ij} are the interaction energy parameters, k_{ij} is the interaction parameter associated with a. The term "c_{ij}" in equation 9 and the term "k_{ij}" in equation 12 are the adjustable parameters in this study.

When the Huron-Vidal mixing rule is applied to PR EOS, the fugacity coefficient of each component for each phase can be calculated by (Zhao & Lvov, 2015):

$$ln\,\varphi_i = \frac{b_i}{b_m}(Z-1) - ln(Z-B) - \frac{1}{2\sqrt{2}}\left(\frac{a_i}{b_i RT} + \frac{ln\,\gamma_i}{A}\right) ln\left(\frac{Z+(1+\sqrt{2})B}{Z-(1+\sqrt{2})B}\right) \tag{13}$$

where Z is the compressibility factor and can be solved by equation 14:

$$Z^3 - (1-B)Z^2 + (A - 3B^2 - 2B)Z - (AB - B^2 - B^3) = 0 \tag{14}$$

where

$$A = \frac{a_m p}{R^2 T^2} \tag{15}$$

$$B = \frac{b_m p}{RT} \tag{16}$$

In equation 13, $ln\,\gamma_i$ is the activity coefficient of the component i in the NRTL model, which can be found from Wong & Sandler (1992):

$$ln\,\gamma_i = \frac{\sum_{j=1}^{n} \frac{C_{ji}}{RT} z_j b_j G_{ji}}{\sum_{k=1}^{n} z_k G_{ki}} + \sum_{j=1}^{n}\left[\frac{z_j G_{ij}}{\sum_{k=1}^{n} z_k G_{kj}}\left(\frac{C_{ij}}{RT} - \frac{\sum_{l=1}^{n} z_l \frac{C_{li}}{RT} G_{lj}}{\sum_{k=1}^{n} z_k G_{kj}}\right)\right] \tag{17}$$

2.3 Data Collection

Table 1 summarizes the experimental data related to the phase equilibria of CO_2+salt(s)+H_2O systems that are available in the literature. The collected data cover a wide range of temperature, pressure, and molality, which can well represent the typical geological conditions (172-523.15 K, 0-596 bar, and 0-6 mol/kg).

Table 1. Experimental VLE data of CO_2+salt(s)+H_2O systems in the literature.

***T*/K**	***P*/bar**	x_{CO_2}[a]	y_{CO_2}[b]	**NDP**	**Salts**	**Authors**
322-373	17-230	0.237-1.700	-	21	NaCl	Chabab et al.
323-413	50-400	0.342-2.569	-	36	NaCl	Koschel et al.
323-423	50-202	2.302-11.02	-	36	NaCl	Messabeb et al.
308-413	99-358	0.662-2.116	-	16	NaCl	Gilbert et al.
273-473	100-400	0.561-3.065	-	180	NaCl	Guo et al.
323-423	150	0.698-1.797	-	36	NaCl	Zhao et al.
323-353	1-213	0.007-2.159	-	49	NaCl	Mohammadian et al.
323-423	26-182	0.195-1.335	81.4-99.9	36	NaCl	Hou et al.
423	125-341	0.911.578-	-	7	NaCl	Savary et al.
323 -373	51-200	0.43-1.81	-	14	NaCl	Koschel et al.
333-333	100-200	1.65-2.46	-	36	NaCl	Bando et al.
313-353	0.1-101	0-0.0038	-	66	NaCl	Kiepe et al.
313-433	1.5-90	0-0.981	-	69	NaCl	Rumpf et al.
353-473	21.1-100	0.28-1.54	-	34	NaCl	Nighswander et al.
445-598	27-93	0.318-1.84	-	39	NaCl	Ellis & Golding
323-523	82-548	1.2-2.52	-	26	KCl	Teymouri
297	21-172.3	0.822-2.374	-	21	KCl	Jacob & Saylor
323-423	150	1.008-1.779	-	16	KCl	Zhao, Dilmore, et al.

323-423	29.2-181	0.552-1.282	81.1-99.8	36	KCl	Hou et al.
318.15	21-158	0.607-1.736	-	8	KCl	Liu et al.
313-433	3 -94	0-1.572	-	102	KCl	Kamps et al.
313-353	0.07-95	0-2.174	-	96	KCl	Kiepe et al.
273-363	0.3-1	0.005-0.128	-	26	KCl	He & Morse
323-423	80-596	0.66-1.78	-	39	$CaCl_2$	Teymouri
323-423	150	0.79-1.933	-	18	$CaCl_2$	Zhao, Dilmore, et al.
328-375	69-207	0.3-1.03	-	22	$CaCl_2$	Bastami et al.
309-424	15.3-424	0.14-1.61	-	36	$CaCl_2$	Tong et al.
318.15	21-159	0.519-1.505	-	8	$CaCl_2$	Liu et al.
348-394	15-874	0.17-2.12	-	130	$CaCl_2$	Prutton & Savage
323-423	150	0.596-3.478	-	18	$MgCl_2$	Zhao, Dilmore, et al.
310-425	13-349	0.13-1.75	-	39	$MgCl_2$	Tong et al.
273-363	0.301-0.966	0.004-0.126	-	27	$MgCl_2$	He & Morse
309-425	10-171	0.3-1.58	-	14	NaCl+KCl	Tong et al.
318.15	25-160	0.636-1.603	-	8	NaCl+KCl	Liu et al.
323-423	10-199	0.067-1.780	-	24	NaCl+$CaCl_2$	Poulain et al.
318.15	25-160	0.594-1.496	-	8	NaCl+$CaCl_2$	Liu et al.
318.15	21-159	0.561-1.646	-	8	KCl+$CaCl_2$	Liu et al.
308-328	21-159	0.378-2.012		72	NaCl+KCl+$CaCl_2$	Poulain et al.
323-423	10-200	0.067-1.744		24	NaCl+KCl+$CaCl_2$	Liu et al.
323-423	100-571	0.82-1.48	-	18	NaCl+KCl+$CaCl_2$+$MgCl_2$	Teymouri

a: Molar concentration of CO_2 in the aqueous phase.
b: Molar concentration of CO_2 in the gas phase.

2.4 Objective Functions and Errors

All the collected experimental data can be categorized into three forms: (1) *T-P-x*; (2) *T-P-y*; and (3) *T-P-x-y*. All the data mentioned above were used for BIP optimization. The parameterization of the model in this work consists of two parameters (*c, k*). The optimization of these two parameters is carried out by minimizing the objective functions given below. The form of the objective function depends on the category of the data employed in the optimization. When only the aqueous phase data are available, the BIP determination is carried out by minimizing the following objective function:

$$F = \sum_{i=1}^{NDP} \sum_{j=1}^{n} \left| \frac{x_{j,i}^{\exp} - x_{j,i}^{cal}}{x_{j,i}^{\exp}} \right| \tag{18}$$

When only the gas phase data are available, the following objective function is applied:

$$F = \sum_{i=1}^{NDP} \sum_{j=1}^{n} \left| \frac{y_{j,i}^{\exp} - y_{j,i}^{cal}}{y_{j,i}^{\exp}} \right| \tag{19}$$

When both aqueous and gas phase data are available, the following objective function is applied:

$$F = \sum_{i=1}^{NDP} \sum_{j=1}^{n} \left[\left| \frac{x_{j,i}^{\exp} - x_{j,i}^{cal}}{x_{j,i}^{\exp}} \right| + \left| \frac{y_{j,i}^{\exp} - y_{j,i}^{cal}}{y_{j,i}^{\exp}} \right| \right] \tag{20}$$

where *n* represents the number of components in the mixture, *NDP* corresponds to the number of data points, $x_{j,i}^{exp}$ and $x_{j,i}^{cal}$ represents the experimental and calculated mole fraction of CO_2 or H_2O in the aqueous phase, respectively; $y_{j,i}^{exp}$ and $y_{j,i}^{cal}$ are the measured and calculated mole fraction of CO_2 or H_2O in the gas phase, respectively. Once we obtain the discrete *k* values that are optimized

based on the experimental data, we adopt the linear regression method to obtain the correlations of k vs. temperature and k vs. molality. Once the c and k are evaluated, the CO_2 solubility in the aqueous phase and H_2O content in the gas phase can be calculated with the aforementioned thermodynamic framework. The modeling results of CO_2 contents in the aqueous and H_2O contents in the gas phase are compared to the experimental data in terms of average absolute percentage deviation (*%AAD*), average absolute deviation (*AAD*):

$$\%AAD = \frac{100}{NDP}\sum_{i=1}^{NDP}\left|\frac{x_{cal} - x_{exp}}{x_{exp}}\right|_i \tag{21}$$

$$AAD = \frac{1}{NDP}\sum_{i=1}^{NDP}\left|x_{exp} - x_{cal}\right|_i \tag{22}$$

where x_{cal} denotes the calculated CO_2 solubility values in this study, and x_{exp} represents the experimental CO_2 solubility taken from the literature.

2.5 Model Evaluation

2.5.1 CO_2+Single-Salt+H_2O Systems

The two BIPs (i.e., c and k) in the Huron-Vidal mixing rule can be constant values or temperature-dependent functions for the pure CO_2+H_2O system. However, for CO_2+mixed-salt+H_2O systems, the BIPs can be significantly affected by the type and molality of different salts.

In this research, four BIP strategies are tried to find out the optimal BIP strategy for CO_2+single-salt+H_2O systems. In the following discussion, we use the CO_2+NaCl+H_2O system as an example to demonstrate how to determine the optimal BIP strategies for the CO_2+single-salt+H_2O systems. The next step is to develop a mixing rule for predicting the BIP such that the model can be extended

to CO_2+mixed-salt+H_2O systems. **Table 2** lists the four different strategies adopted to optimize the BIPs in the Huron-Vidal mixing rule for CO_2+single-salt+H_2O systems.

Table 2. Different strategies used for optimizing the BIPs in the Huron-Vidal mixing rule in PR EOS for CO_2+single-salt+H_2O systems.[a]

Case #	BIP Strategy	Description
1	c=constant; k=constant	c and k are determined as constant values over the entire database[a].
2	c=varying constant; k=varying constant	c and k are optimized at each data point (each temperature, pressure, and molality combination)[b].
3	c=constant; k=varying constant	c is optimized as a constant value over the entire database [b]; k is optimized at each data point (each temperature, pressure, and molality combination)[c].
4	c=constant, $k=k$ (T, M)	c is optimized as a constant over the entire database[a]; k is first optimized at each data point and then regressed as a function of temperature and molality[d].

a: The BIP strategies in this work are similar to the strategies used by (Abudour et al., 2012) and (Yin et al., 2020).
b: The BIP values are determined by a global optimization approach: c and k are only two constant values that are optimized for all temperatures and molality levels.
c: The BIP values are determined by using the following optimization method: c and k are specific values that are optimized at each data point; c and k are independent of temperature and molality.
d: c is the same constant value for all temperatures and molality levels; k varies with temperature and molality.

As shown in **Table 2**, four cases are investigated to determine the optimal BIP strategy for the CO_2+single-salt+H_2O systems:

In Case 1, both c and k are globally optimized as constant values over the entire database by employing the objective functions in equations 18-20. In Case 1, c and k are independent of temperature, pressure, and molality.

In Case 2, the strategy used in Case 1 is improved: c and k are optimized as a constant value for each data point, independent of temperature and molality. **Figure 1** shows the optimized results for the CO_2+NaCl+H_2O system in Case 2. Specifically, **Figure 1a** and **Figure 1b** show the distribution of the optimal c values versus temperature and molality, respectively; **Figure 1c** and **Figure 1d** show the distribution of the optimal k values versus temperature and molality, respectively. As seen, both optimal c and k values are scattered values. Since there is no clear trend of c and k versus temperature and molality, the BIPs in Case 2 cannot be generalized. Hence, there is no point to discuss the errors yielded by Case 2.

In Case 3, the globally optimized c value is found to be 0.04, then the k values are optimized once c is set as a constant. Note that c is independent of temperature and molality. Since c is a single, constant value, this allows the variation of optimal k with temperature and molality. **Figure 3** shows the trend of optimal k values versus temperature and molality in Case 3. As seen in **Figure 2a**, the CO_2+single-salt+H_2O system shows a clear molality-dependence of k. Similar to **Figure 2b**, there is a linear relationship between k and temperature. Note that in **Figure 2b**, there are 5 outliers because the k values of those outliers are much lower than the others. Therefore, later in the regression process, these outliers are discarded. Again, since the BIP expression in Case 3 cannot be generalized, here we don't discuss the errors yielded by Case 3.

In Case 4, we use the same optimal c value as used in Case 3. We try to use quadratic relationships of k vs. temperature (T) and k vs. molality (M). The three-dimensional k-T-M plots for the specific CO_2+single-salt+H_2O systems are illustrated in **Figure 3**. As seen from **Figure 3**, a quadratic equation, as expressed by equation 25 seems to work well in describing the relationship k=k (T, M).

Note that to find the optimal BIP strategy for the other three CO_2+single-salt+H_2O systems (KCl, $CaCl_2$, $MgCl_2$) below, we use the same constant c value as used in Case 4. Using the objective functions defined by equations 18-20, all the values and expressions of BIPs in each CO_2+single-salt+H_2O system are obtained by the same optimization methodology as mentioned above.

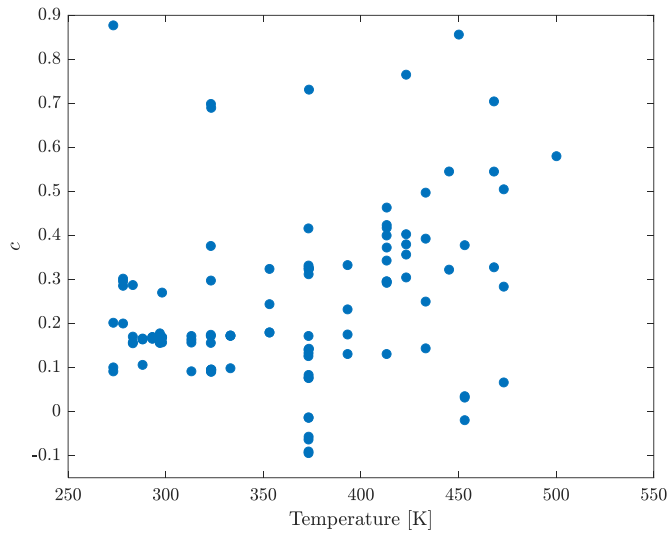

(a)

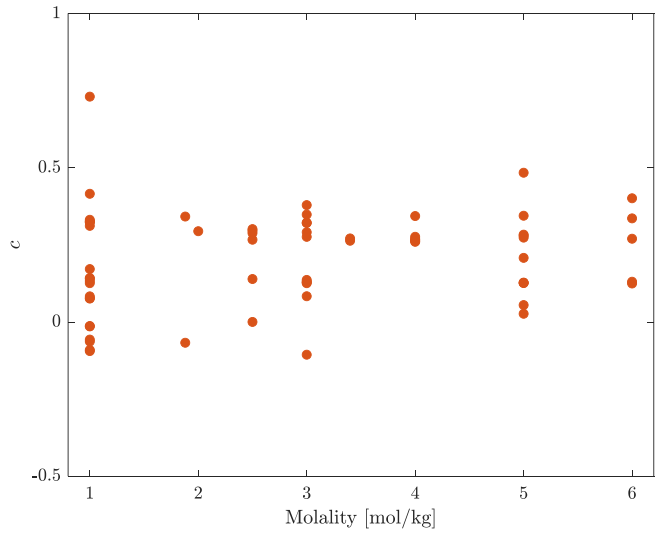

(b)

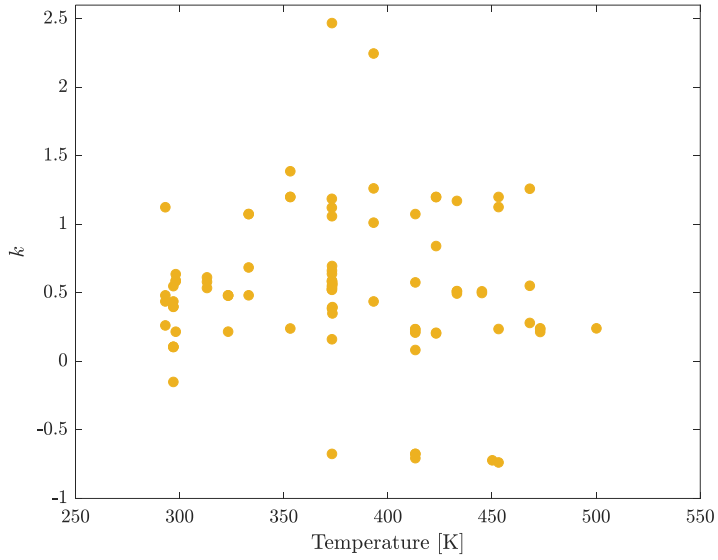

(c)

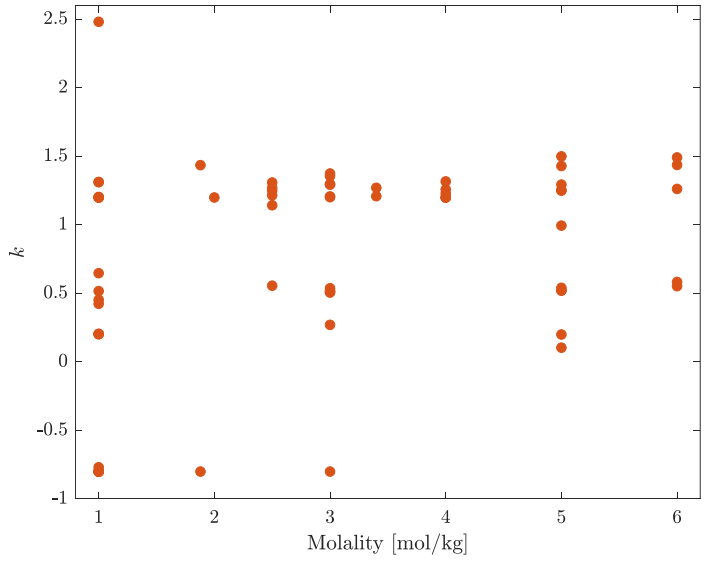

(d)

Figure 1. Plots of optimal *c* and *k* values versus temperature and molality for CO_2+NaCl+H_2O system in Case 2: (a) optimal *c* values versus temperature; (b) optimal *c* values versus molality; (c) optimal *k* values versus temperature; (d) optimal *k* values versus molality.

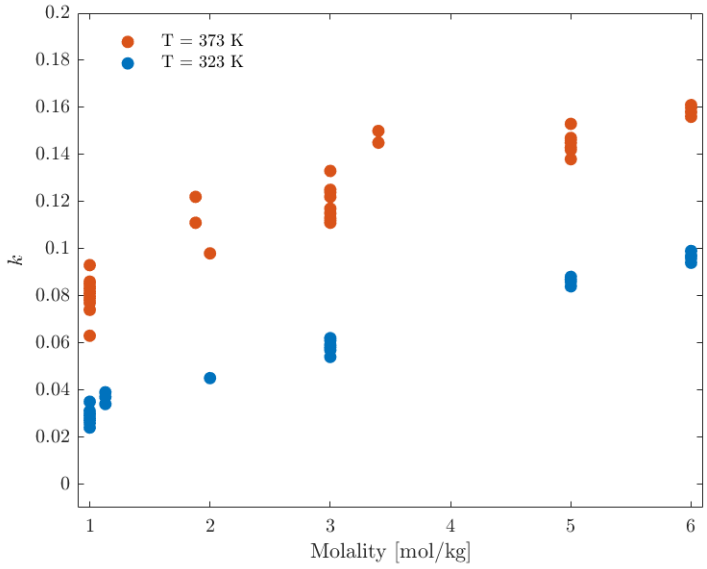

(a)

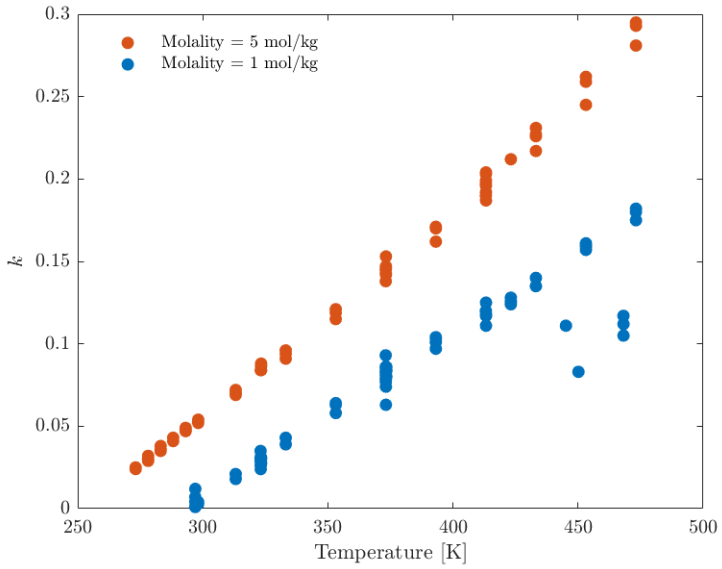

(b)

Figure 2. Influence of temperature and NaCl molality on optimal k in Case 3: (a) optimal k values versus molality; (b) optimal k values versus temperature.

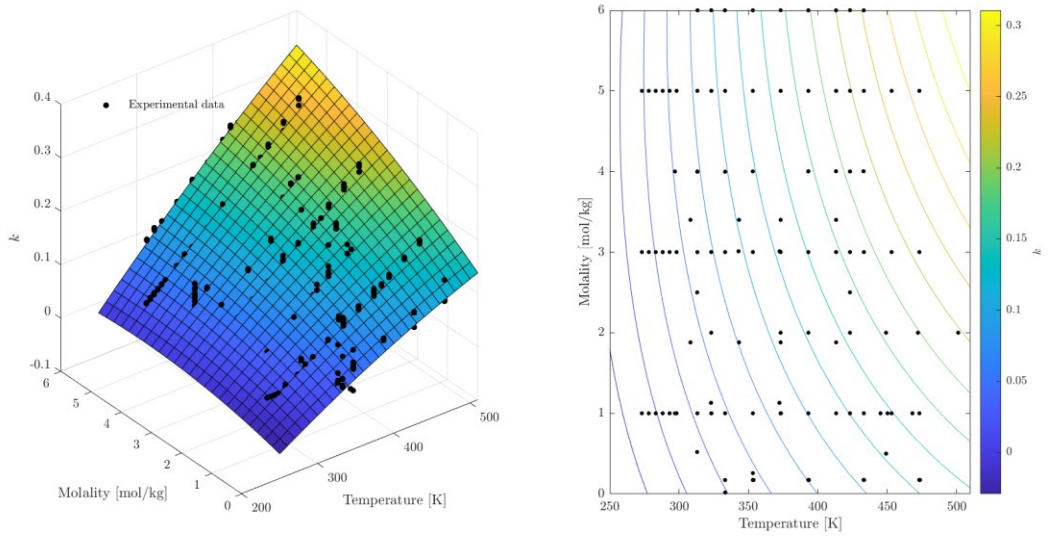
Experimental data
k
Molality [mol/kg]
Temperature [K]
Molality [mol/kg]
Temperature [K]
k

(a)

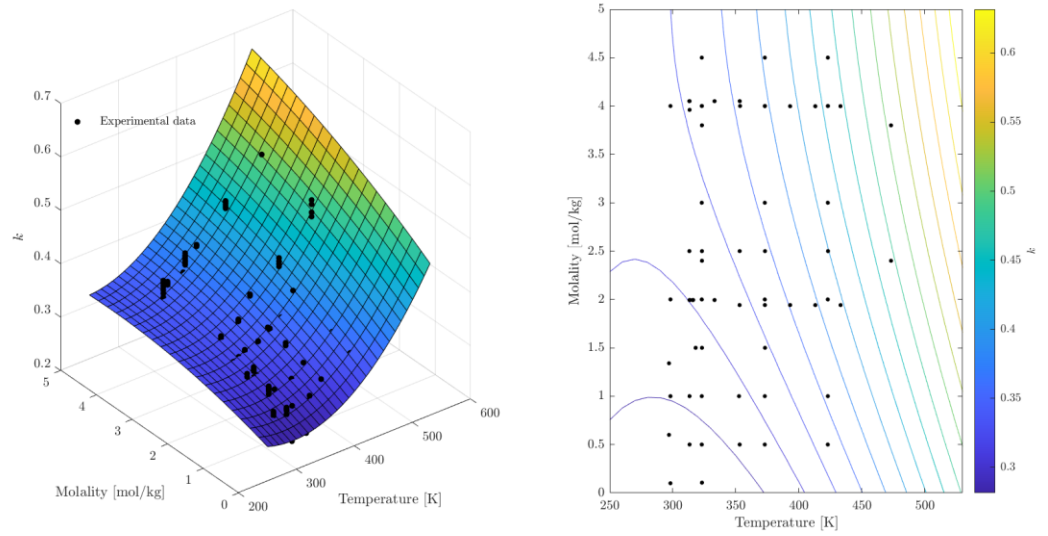
Experimental data
k
Molality [mol/kg]
Temperature [K]
Molality [mol/kg]
Temperature [K]
k

(b)

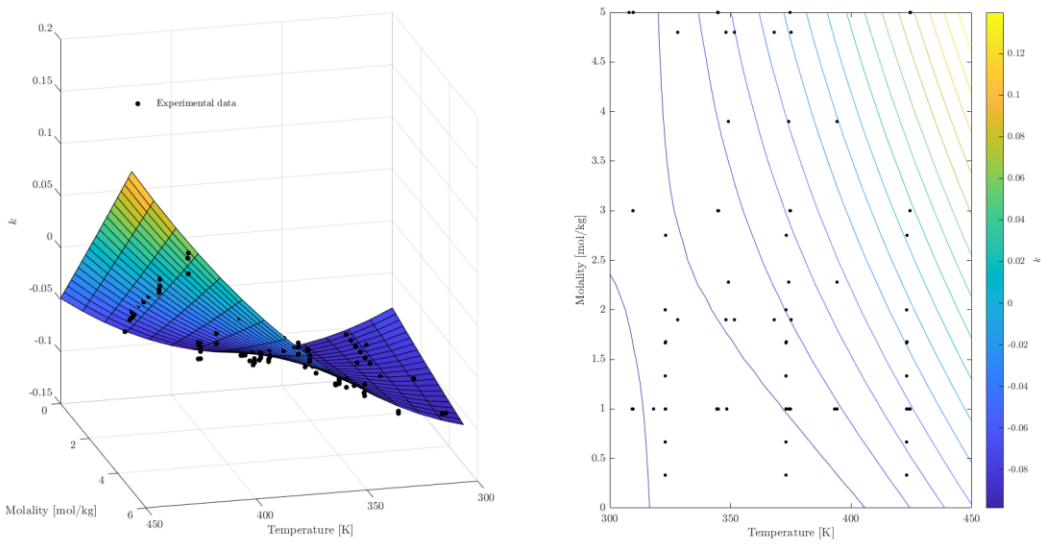

(c)

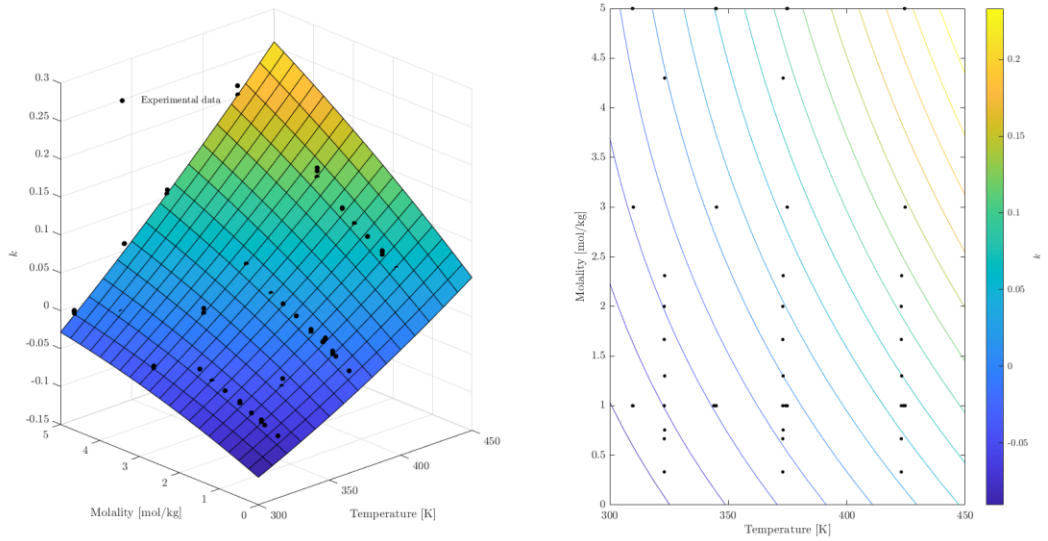

(d)

Figure 3. Plots of optimal k values versus temperature and molality for CO_2+single-salt+H_2O systems in Case 4: (a) CO_2+NaCl+H_2O system; (b) CO_2+KCl+H_2O system; (c) CO_2+$CaCl_2$+H_2O system; (d) CO_2+$MgCl_2$+H_2O system.

2.5.2 Extension of the Model to CO_2+Mixed-Salt+H_2O Systems

We can perform a similar analysis for brine mixtures composed of mixed salts. The following model is established to predict the *k* value for brine mixtures (k_{mix}). Considering N salts in a brine mixture, a prediction model for calculating the *k* value is proposed by considering the contributions of different types of salts:

$$k_{mix} = \sum_{i=1}^{N} \alpha_i^{a_i} \frac{M_i}{\sum_{i=1}^{N} M_j + \epsilon} k_i + C \tag{23}$$

where

$$a_i = \frac{\sum_{i=1}^{N} M_j - M_i}{M_i} \tag{24}$$

$$k_i = aT^2 + bM_i^2 + dTM_i + eT + fM_i + g \tag{25}$$

where k_{mix} represents the *k* value of a brine mixture; i indicates the i_{th} salt species in the mixed-salt solution; M_i is the molality of the i_{th} salt species, mol/kg; a-g represents the regression coefficients obtained for a given CO_2+single-salt+H_2O system; $(\alpha_i, i = 1, \dots N)$ are the regressed coefficients representing the contributions of different salts; *C* is a regressed constant; ϵ is a very small number and set to be 10^{-10} in this study.

For example, if there are only 2 salts in the brine mixture, equation 23 reduces to:

$$k_{mix} = \alpha_1^{\frac{M_2}{M_1}} \frac{M_1}{M_1 + M_2} k_1 + \alpha_2^{\frac{M_1}{M_2}} \frac{M_2}{M_1 + M_2} k_2 + C \tag{26}$$

2.6 Two-Phase Flash Calculation

For a given pressure, temperature and feed composition, two-phase flash calculation is used to determine the number of phases and the composition of each of these phases (Whitson & Brulé, 2000). This calculation consists of using material-balance and equal-fugacity constraints and numerical methods such as successive-substitution iteration or Newton Raphson algorithm. These constraints imply thermodynamic equilibrium, i.e., the chemical potential of a particular component in each phase must be the same. Mathematically, this can be expressed as:

$$f_{Li} = f_{Vi}, i = 1, \dots, N \tag{27}$$

where f_{Li} and f_{Vi} are the fugacity coefficients of the i_{th} component in liquid phase and gas phase, respectively. To satisfy these constraints, the Rachford-Rice equation (Rachford & Rice, 1952) is solved, i.e.,

$$h(F_v) = \sum_{i=1}^{n} \frac{z_i(K_i - 1)}{1 + F_v(K_i - 1)} = 0 \tag{28}$$

where F_v is the vapor phase mole fraction; K_i is the so-called K-value (i.e., gas-liquid equilibrium ratio) and can be written as:

$$K_i = \frac{y_i}{x_i} \tag{29}$$

In this work, a stability test is used to tell whether a given feed is stable or not. The details of the stability test analysis can be found in the studies by Whitson & Brulé (2000) and Michelsen (1982). The initial K-values to initialize the stability test are calculated by (Wilson, 1969):

$$K_i = \frac{\exp[5.37(1 + \omega_i)(1 - T_{ri}^{-1})]}{p_{ri}} \tag{30}$$

where T_{ri} and p_{ri} are the reduced temperature and reduced pressure of the i_{th} component, respectively. Furthermore, to solve for $F_{v,}$ the well-known Newton-Raphson algorithm is used. For more details on the calculation procedure of two-phase flash calculations, the reader is referred to the monograph written by Whitson & Brulé (2000).

References

Abudour, A.M., Mohammad, S.A., & Gasem, K.A.M. (2012). Modeling high-pressure phase equilibria of coalbed gases/water mixtures with the Peng-Robinson equation of state. *Fluid Phase Equilibria*, 319, 77-89.

Bando, S., Takemura, F., Nishio, M., Hihara, E., & Akai, M. (2003). Solubility of CO_2 in aqueous solutions of NaCl at (30 to 60) °C and (10 to 20) MPa. *Journal of Chemical and Engineering Data*, 48(3), 576-579.

Bastami, A., Allahgholi, M., & Pourafshary, P. (2014). Experimental and modelling study of the solubility of CO_2 in various $CaCl_2$ solutions at different temperatures and pressures. *Petroleum Science*, 11(4), 569-577.

Chabab, S., Théveneau, P., Corvisier, J., Coquelet, C., Paricaud, P., Houriez, C., & Ahmar, E.El. (2019). Thermodynamic study of the CO_2-H_2O-NaCl system: Measurements of CO_2 solubility and modeling of phase equilibria using Soreide and Whitson, electrolyte CPA and SIT models. *International Journal of Greenhouse Gas Control*, 91, 102825.

Ellis, A.J., & Golding, R.M. (1963). The solubility of carbon dioxide above 100 degrees C in water and in sodium chloride solutions. *American Journal of Science*. 261(1), 47-60.

Gilbert, K., Bennett, P.C., Wolfe, W., Zhang, T., & Romanak, K.D. (2016). CO_2 solubility in aqueous solutions containing Na^+, Ca^{2+}, Cl^-, SO_4^{2-} and HCO_3^-: The effects of electrostricted water and ion hydration thermodynamics. *Applied Geochemistry*, 67, 59-67.

Guo, H., Huang, Y., Chen, Y., & Zhou, Q. (2016). Quantitative Raman spectroscopic measurements of CO_2 solubility in NaCl solution from (273.15 to 473.15) K at P = (10.0, 20.0, 30.0, and 40.0) MPa. *Journal of Chemical and Engineering Data*, 61(1), 466-474.

He, S., & Morse, J.W. (1993). The carbonic acid system and calcite solubility in aqueous Na-K-Ca-Mg-Cl-SO_4 solutions from 0 to 90°C. *Geochimica Et Cosmochimica Acta*, 57(15), 3533-3554.

Hou, S.X., Maitland, G.C., & Trusler, J.P.M. (2013). Phase equilibria of (CO_2+H_2O+NaCl) and (CO_2+H_2O+KCl): Measurements and modeling. *The Journal of Supercritical Fluids*, 78, 78-88.

Huron, M.J., & Vidal, J. (1979). New mixing rules in simple equations of state for representing vapor-liquid equilibria of strongly non-ideal mixtures, *Fluid Phase Equilibria*, 3, 255-271.

Jacob, R., & Saylor, B.Z. (2016). CO_2 solubility in multi-component brines containing NaCl, KCl, $CaCl_2$ and $MgCl_2$ at 297 K and 1-14 MPa. *Chemical Geology*, 424, 86-95.

Kamps, Á.P.S., Meyer, E., Rumpf, B., & Maurer, G. (2007). Solubility of CO_2 in aqueous solutions of KCl and in aqueous solutions of K_2CO_3. *Journal of Chemical and Engineering Data*, 52(3), 817-832.

Kiepe, J., Horstmann, S., Fischer, K., & Gmehling, J. (2002). Experimental determination and prediction of gas solubility data for CO_2+H_2O mixtures containing NaCl or KCl at

temperatures between 313 and 393 K and pressures up to 10 MPa. *Industrial and Engineering Chemistry Research*, 41(17), 4393-4398.

Koschel, D., Coxam, J. Y., Rodier, L., & Majer, V. (2006). Enthalpy and solubility data of CO_2 in water and NaCl(aq) at conditions of interest for geological sequestration. *Fluid Phase Equilibria*, 247(1-2), 107-120.

Liu, Y., Hou, M., Yang, G., & Han, B. (2011). Solubility of CO_2 in aqueous solutions of NaCl, KCl, $CaCl_2$ and their mixed salts at different temperatures and pressures. *Journal of Supercritical Fluids*, 56(2), 125-129.

Messabeb, H., Contamine, F., Cézac, P., Serin, J.P., & Gaucher, E.C. (2016). Experimental measurement of CO_2 solubility in aqueous NaCl solution at temperature from 323.15 to 423.15 K and pressure of up to 20 MPa. *Journal of Chemical and Engineering Data*, 61(10), 3573-3584.

Michelsen, M.L. (1982) The isothermal flash problem. Part I. Stability. *Fluid Phase Equilibria*, 9, 1-19.

Mohammadian, E., Hamidi, H., Asadullah, M., Azdarpour, A., Motamedi, S., & Junin, R. (2015). Measurement of CO_2 solubility in NaCl brine solutions at different temperatures and pressures using the potentiometric titration method. *Journal of Chemical and Engineering Data*, 60(7), 2042-2049.

Nighswander, J.A., Kalogerakis, N., & Mehrotra, A.K. (1989). Solubilities of carbon dioxide in water and 1 wt. % NaCl solution at pressures up to 10 MPa and temperatures from 80 to 200 °C. *Journal of Chemical and Engineering Data*, 34(3), 355-360.

Peng, D., & Robinson, D.B. (1976). A new two-constant equation of state. *Industrial & Engineering Chemistry Research*, 15(1), 59-64.

Poulain, M., Messabeb, H., Lach, A., Contamine, F., Cézac, P., Serin, J.P., Dupin, J.C., & Martinez, H. (2019). Experimental measurements of carbon dioxide solubility in Na-Ca-K-Cl solutions at high temperatures and pressures up to 20 MPa. *Journal of Chemical and Engineering Data*, 64(6), 2497-2503.

Prutton, C., & Savage, R. (1940). The solubility of carbon dioxide in calcium chloride-water solutions at 75, 100, 120 °C and high pressures. *Journal of the American Chemical Society*, 67(9), 1550-1554.

Rachford Jr, H.H. & Rice, J.D. (1952). Procedure for use of electronic digital computers in calculating flash vaporization hydrocarbon equilibrium. *Journal of Petroleum Technology*, 410, 19-3.

Renon, H., & Prausnitz, J.M. (1968). Local compositions in thermodynamic excess functions for liquid mixtures, *AIChE Journal*, 14(1), 135-144.

Rumpf, B., Nicolaisen, H., Öcal, C., & Maurer, G. (1994). Solubility of carbon dioxide in aqueous solutions of sodium chloride: Experimental results and correlation. *Journal of Solution Chemistry*, 23(3), 431-448.

Savary, V., Berger, G., Dubois, M., Lacharpagne, J.C., Pages, A., Thibeau, S., & Lescanne, M. (2012). The solubility of CO_2+H_2S mixtures in water and 2M NaCl at 120 °C and pressures up to 35 MPa. *International Journal of Greenhouse Gas Control*, 10, 123-133.

Sørensen, H., Pedersen, K.S., & Christensen, P.L. (2002). Modeling of gas solubility in brine. *Organic Geochemistry*, 33(6), 635-642.

Teymouri, S. (2017). Phase equilibria measurements and modelling of CO_2-rich fluids/brine system*s*, Doctoral dissertation, Heriot-Watt University.

Tong, D., Trusler, J. P. M., & Vega-Maza, D. (2013). Solubility of CO_2 in aqueous solutions of $CaCl_2$ or $MgCl_2$ and in a synthetic formation brine at temperatures up to 423 K and pressures up to 40 MPa. *Journal of Chemical and Engineering Data*, 58(7), 2116-2124.

Whitson, C.H., & Brulé, M.R. (2000). Phase behavior. SPE Monograph.

Wilson, G.M. (1969). Modified Redlich-Kwong equation of state, application to general physical data calculations. *65th National AIChE Meeting*, Cleveland, OH, 15.

Wong, D.S.H., & Sandler, S.I. (1992). A theoretically correct mixing rule for cubic equations of state. *AIChE Journal*, 38(5), 671-680.

Yin, S., Wang, Z., Lu, C., & Li, H. (2020). Towards accurate phase behavior modeling for hydrogen sulfide/water mixtures. *Fluid Phase Equilibria*, 521, 112691.

Zhao, H., Dilmore, R. M., & Lvov, S.N. (2015). Experimental studies and modeling of CO_2 solubility in high temperature aqueous $CaCl_2$, $MgCl_2$, Na_2SO_4, and KCl solutions. *AIChE Journal*, 61(7), 2286-2297.

Zhao, H., Fedkin, M.V., Dilmore, R.M., & Lvov, S.N. (2015). Carbon dioxide solubility in aqueous solutions of sodium chloride at geological conditions: Experimental results at 323.15, 373.15, and 423.15 K and 150 bar and modeling up to 573.15 K and 2000 bar. *Geochimica Et Cosmochimica Acta*, 149, 165-189.

Zhao, H., & Lvov, S.N. (2016). Phase behavior of the CO_2-H_2O system at temperatures of 273-623 K and pressures of 0.1-200 MPa using Peng-Robinson-Stryjek-Vera equation of state with a modified Wong-Sandler mixing rule: an extension to the CO_2-CH_4-H_2O system. *Fluid Phase Equilibria*, 417, 96-108.

CHAPTER 3 RESULTS AND DISCUSSION

3.1 Determination of the Optimal BIP Strategy

3.1.1 Optimal BIP Strategy for CO_2+Single-Salt+H_2O Systems

In the following discussion, since the concentration of CO_2 in brine is very small, *%AAD* (equation 21) and *AAD* (equation 22) are considered as indices to evaluate the performance of the different BIP strategies (cases). The values of these indices are shown in **Table 3** for the CO_2+NaCl+H_2O system. Notice that Case 1, where optimal c and k have values of 0.15 and 0.62, respectively, exhibits the largest error in reproducing CO_2 concentration in the aqueous phase (x_2); it yields 40.31*%AAD* in x_2 calculations and 45.32*%AAD* in y_1 calculations.

Table 3. Summary of the errors yielded by the different BIP strategies for CO_2+NaCl+H_2O system by different BIP strategies.[a]

Case #	BIP Strategy	Molar fraction of CO_2 in the liquid phase (x_2)		Molar fraction of H_2O in the vapor phase (y_1)	
		%AAD	*AAD*10³*	*%AAD*	*AAD*10³*
1	c=0.15; k=0.62	40.31	12.10	45.32	6.11
2	c=varying constant; k= varying constant	-	-	-	-
3	c=0.04; k= varying constant	-	-	-	-
4	c=0.04; k=k (T, M)	9.27	0.94	20.4	11.5

a: In this work, the BIP strategies applied in this study are similar to the BIP strategies used by Abudour et al. (2012) and Yin et al. (2020).

As for Case 2, both c and k values are individually optimized for each isotherm and molality combination. As a consequence, this will offer a much better performance than Case 1 but there is no specific form of the generalized expression of c. As explained in Chapter 2, Section 2.5, the distribution of optimal c values versus temperature or molality is quite scattered, but there is a

clear trend between the optimal *k* and temperature, as well as a clear trend between the optimal *k* and molality. This finding reveals that *k* is dependent on temperature and molality, and it increases with temperature and molality. However, as explained before, since the expression of BIPs in Cases 2 and Case 3 cannot be generalized, here we do not discuss their performance. But the findings given by Case 2 and Case 3 serve as inspirations for Case 4.

As for Case 4, the optimal *c* value is a constant value of 0.04, while the optimal *k* value is regressed as a function of temperature and molality. In this case, it yields 9.27*%AAD* and 0.00094*AAD* in reproducing x_2. Moreover, compared to Case 1, Case 4 yields a higher accuracy in reproducing x_2, i.e., 9.27*%AAD vs* 40.31*%AAD.* Therefore, the BIP strategy obtained in Case 4 can be considered to be the optimal BIP strategy for the CO_2+NaCl+H_2O system. Optimal *c* values in Case 4 considering the other three salt systems (KCl, $CaCl_2$, and $MgCl_2$) can be found in **Table 4**.

Table 4. Optimal *c* values for different CO_2+salt(s)+H_2O systems.

Systems	***c***
CO_2+mixed-salts+H_2O	-0.0011
CO_2+NaCl+H_2O	0.0400
CO_2+KCl+H_2O	0.0200
CO_2+$CaCl_2$+H_2O	-0.0500
CO_2+$MgCl_2$+H_2O	-0.0500

When c is kept at a constant value, the expression for estimating k for each considered CO_2+single-salt+H_2O system is as follows:

$$k = aT^2 + bM^2 + dTM + eT + fM + g \tag{31}$$

where T is temperature in K, M is molality in mol/kg, and the coefficients a-f are found using regressions. The values of these coefficients for each salt system are shown in **Table 5**. Notice that in all the four cases, the coefficients corresponding to the linear terms of T and M are zero.

Table 5. The values of the coefficients appearing in equation 31.

Systems	$k = aT^2 + bM^2 + dTM + eT + fM + g$					
	a	b	d	e	f	g
CO_2+NaCl+H_2O	-0.324	0.001	-0.009	0	0	-0.002
CO_2+KCl+H_2O	-0.224	0	-0.008	0	0	-0.001
CO_2+$CaCl_2$+H_2O	-0.341	0	-0.012	0	0	-0.002
CO_2+$MgCl_2$+H_2O	-0.237	0	-0.024	0	0	-0.001

3.1.2 Extension of the BIP Correlations to CO_2+Mixed-Salts+H_2O Systems

The results presented above are extended to CO_2+mixed-salts+H_2O systems. This is done by using a mixing rule model to calculate k_{mix} by considering the contributions of individual salts as shown in equation 23. This equation is only applicable to the mixed-salt systems, of which its coefficients are found using the data shown in **Table 1** and applying non-linear regression strategies; the regression results are shown in **Table 6**.

Table 6. Optimized parameters in the k_{mix} expression for the CO_2+mixed-salts+H_2O systems.

Coefficients				
α_1	α_2	α_3	α_4	C
1	1	1	1	-0.1045

The performance of equation 23 is summarized in **Table 7** which shows the values of *%AAD* and *AAD* yielded by using the k_{mix} correlation for different systems. As shown in **Table 7**, the proposed

model can well predict VLE of the four CO_2+single-salt+H_2O systems. Note that the proposed model gives the highest accuracy for the CO_2+$MgCl_2$+H_2O system among the above four systems.

Table 7. *%AAD* and *AAD* exhibited by using the k_{mix} correlation in reproducing x_2 and y_1 for different systems.

System	Molar fraction of CO_2 in the liquid phase (x_2)		Molar fraction of H_2O in the vapor phase (y_1)	
	%AAD	*AAD*10³*	*%AAD*	*AAD*10³*
CO_2+mixed-salts-H_2O	7.63	1.46	-	-
CO_2+NaCl+H_2O	9.27	0.94	20.4	11.5
CO_2+KCl+H_2O	6.10	0.48	6.78	0.58
CO_2+$CaCl_2$+H_2O	11.99	0.97	-	-
CO_2+$MgCl_2$+H_2O	4.21	0.37	-	-

3.2 Performance of the Optimal BIP Strategy in Reproducing VLE Data

3.2.1 Model Performance for Single-Salt Brine Systems

In this section, first, the comparison of the reproduced x_2 and y_1 using the optimal BIP strategy (Case 4) against the calculated ones is discussed. Secondly, the reproduced x_2 for the NaCl brine system is compared with that predicted by Søreide & Whitson (1992) and Sun et al. (2021). The former represents one of the first efforts for the estimation of CO_2 solubility in NaCl brine system, while the latter represents a newly proposed method that has shown a good accuracy. As for the other three single-salt systems (KCl, $CaCl_2$, and $MgCl_2$), we only compare the proposed models to the model developed by Sun et al. (2021), since the Søreide & Whitson (1992) model is only applicable to NaCl brines.

CO_2 Fraction in the Aqueous Phase

Figure 4-7 shows the performance of the optimal BIP strategy in reproducing x_2 for each CO_2+single-salt+H_2O system, i.e., CO_2+NaCl+H_2O (**Figure 4**), CO_2+KCl+H_2O (**Figure 5**),

CO_2+$CaCl_2$+H_2O (**Figure 6**), and CO_2+$MgCl_2$+H_2O (**Figure 7**). In general, the developed model exhibits a good performance at pressures up to 300 bar over a temperature range of 323-423 K (**Figure 4a**). However, at pressures over 300 bar, the performance of the developed model tends to deteriorate (**Figure 6a**). **Figure 7**, in particular, confirms the results shown in **Table 7** that the optimal BIP strategy exhibits the highest accuracy for the CO_2+$MgCl_2$+H_2O system. For CO_2-single-salt systems, the calculated results demonstrates that the salt species and salinity will significantly influence the CO_2 solubility in the aqueous phase.

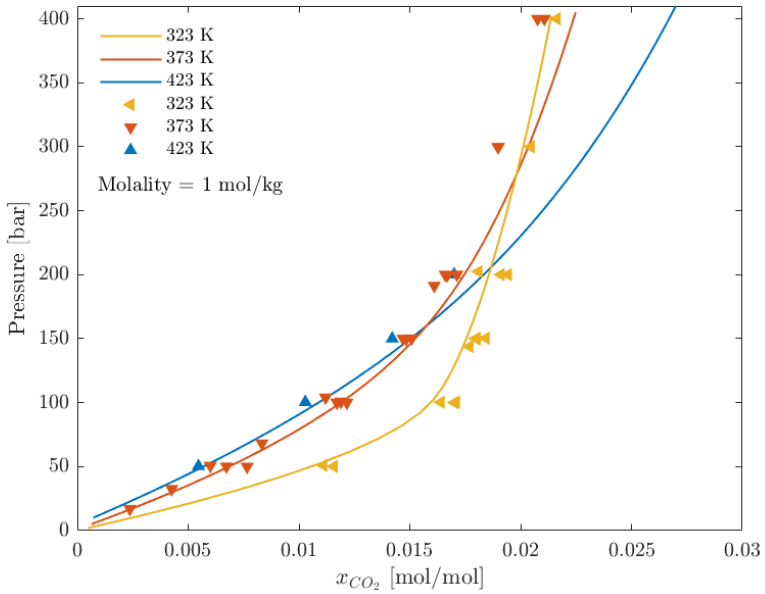

(a)

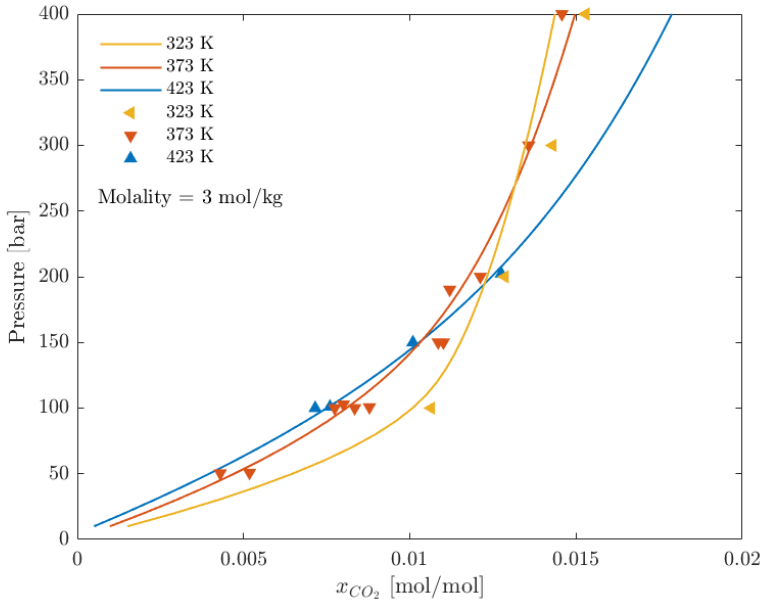
323 K
373 K
423 K
323 K
373 K
423 K
Molality = 3 mol/kg
Pressure [bar]
x_{CO_2} [mol/mol]
0
50
100
150
200
250
300
350
400
0
0.005
0.01
0.015
0.02

(b)

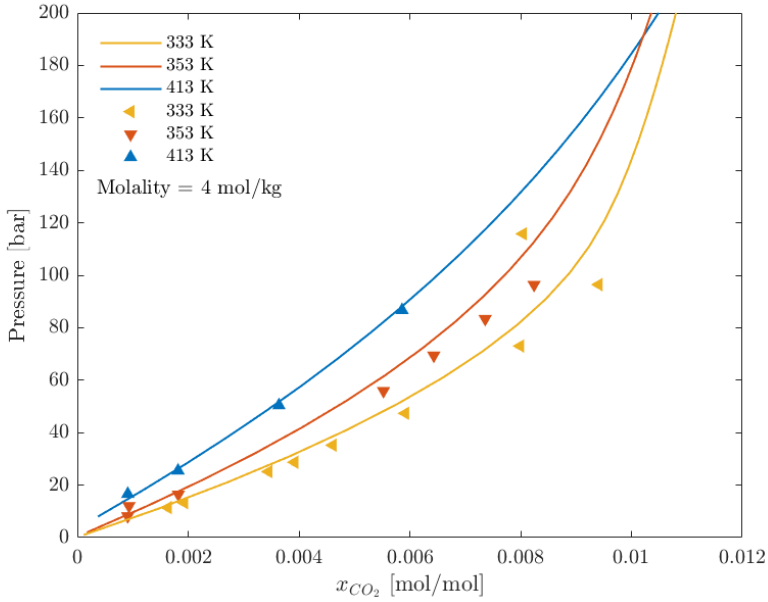
333 K
353 K
413 K
333 K
353 K
413 K
Molality = 4 mol/kg
Pressure [bar]
x_{CO_2} [mol/mol]
0
20
40
60
80
100
120
140
160
180
200
0
0.002
0.004
0.006
0.008
0.01
0.012

(c)

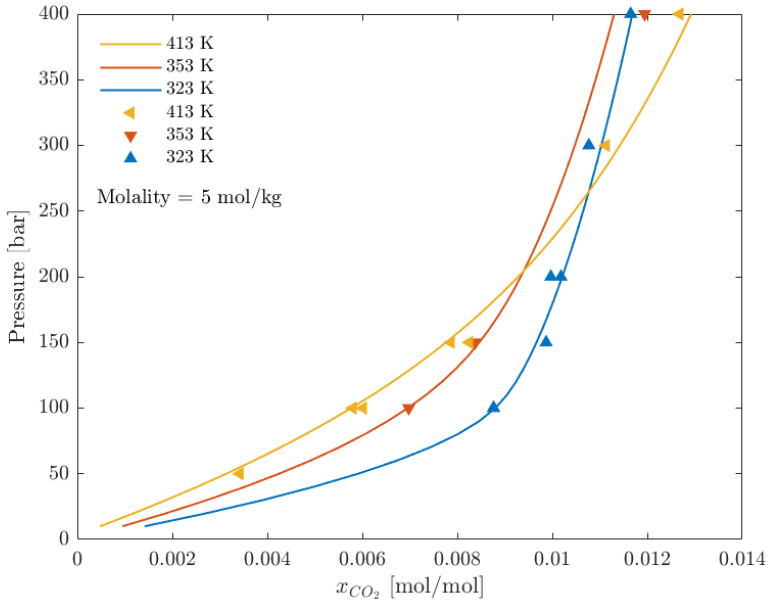

(d)

Figure 4. *p-x* diagram calculated for the CO_2+NaCl+H_2O system: (a) m=1 mol/kg; (b) m=3 mol/kg; (c) m=4 mol/kg; (d) m=5 mol/kg.

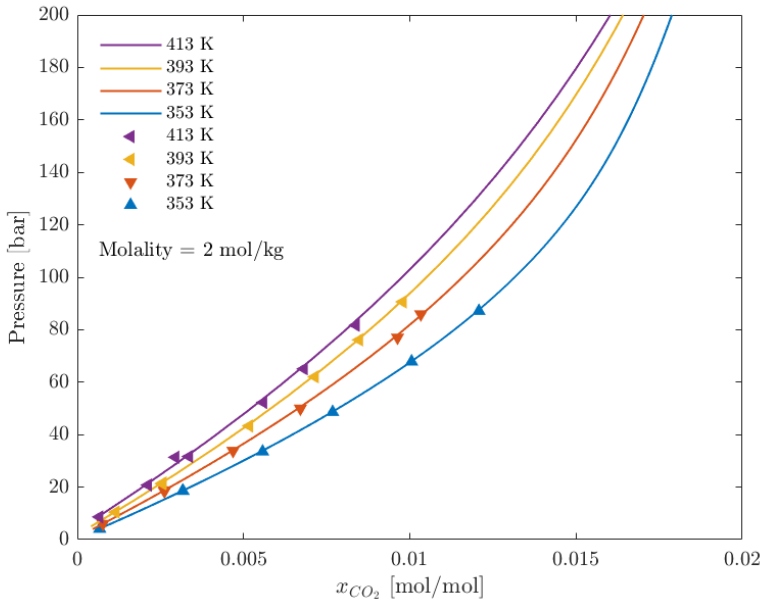

(a)

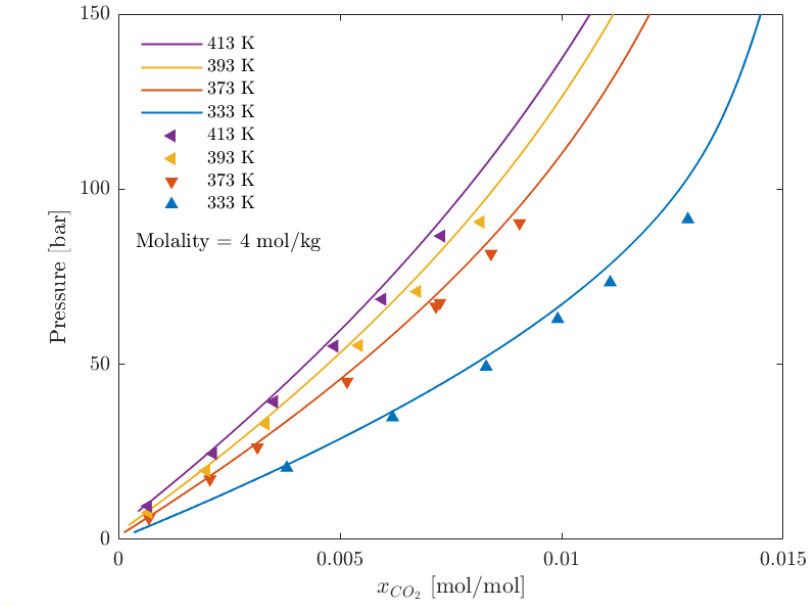

(b)

Figure 5. *p-x* diagram calculated for the CO_2+KCl+H_2O system: (a) m=2 mol/kg; (b) m=4 mol/kg.

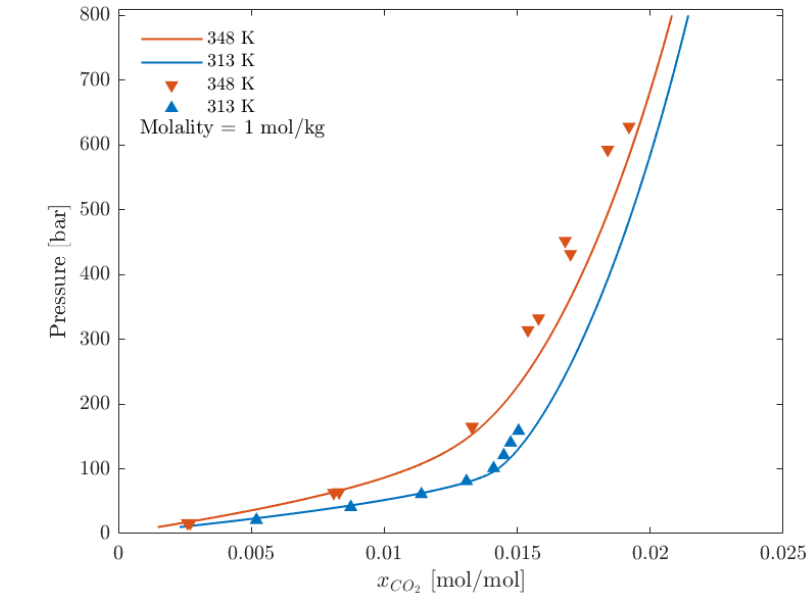

(a)

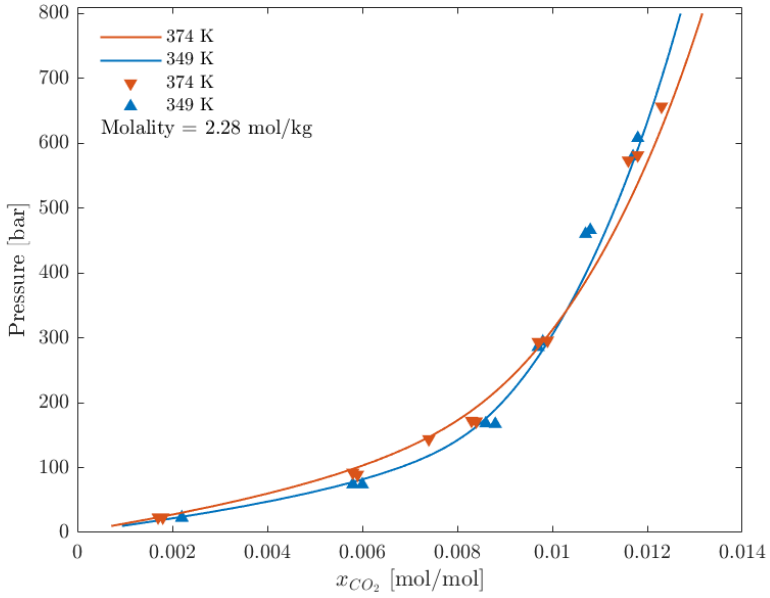

(b)

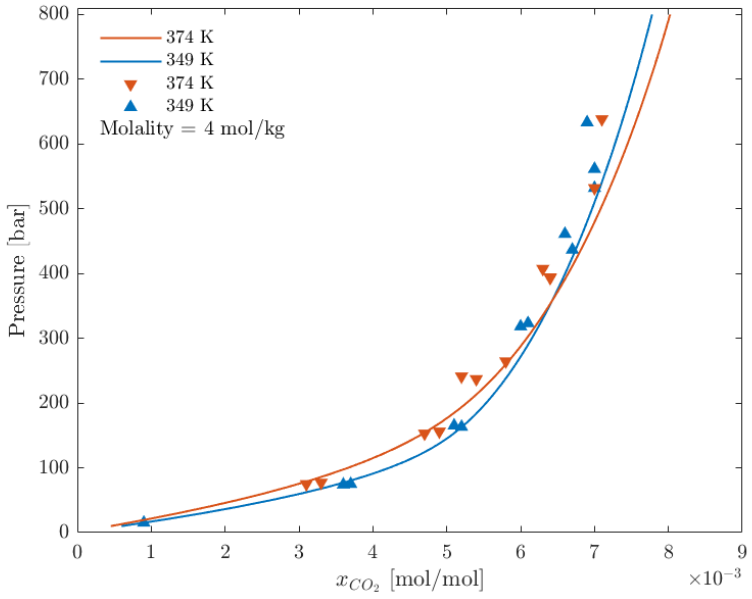

(c)

Figure 6. *p-x* diagram calculated for the CO_2+$CaCl_2$+H_2O system: (a) m=1 mol/kg; (b) m=2.28mol/kg; (c) m=4 mol/kg.

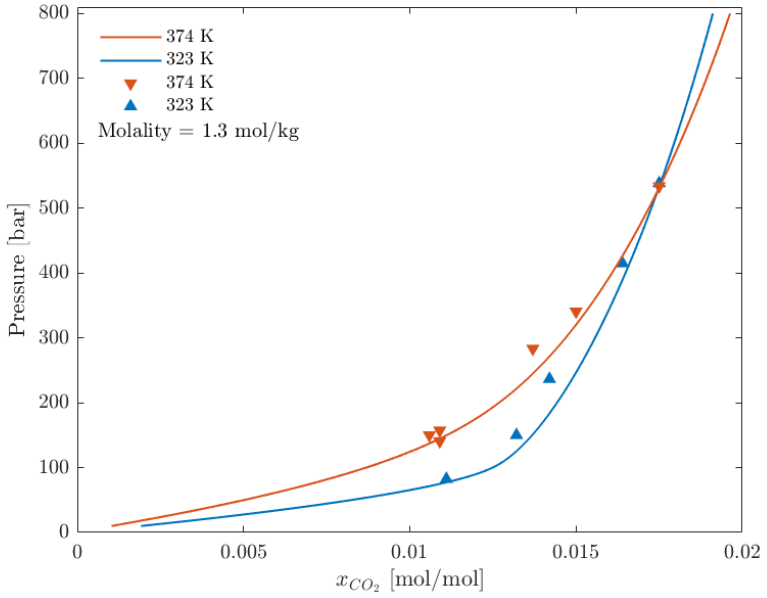
374 K
323 K
374 K
323 K
Molality = 1.3 mol/kg
Pressure [bar]
x_{CO_2} [mol/mol]
0
100
200
300
400
500
600
700
800
0
0.005
0.01
0.015
0.02

(a)

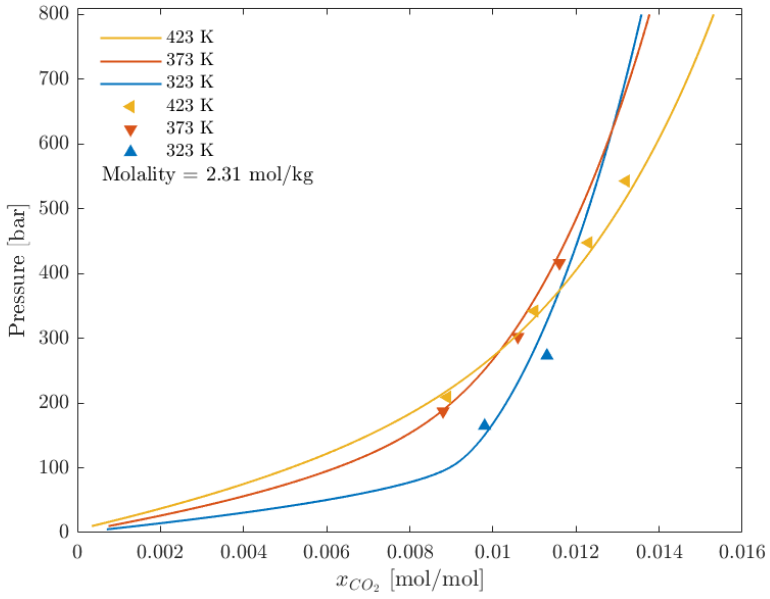
423 K
373 K
323 K
423 K
373 K
323 K
Molality = 2.31 mol/kg
Pressure [bar]
x_{CO_2} [mol/mol]
0
100
200
300
400
500
600
700
800
0
0.002
0.004
0.006
0.008
0.01
0.012
0.014
0.016

(b)

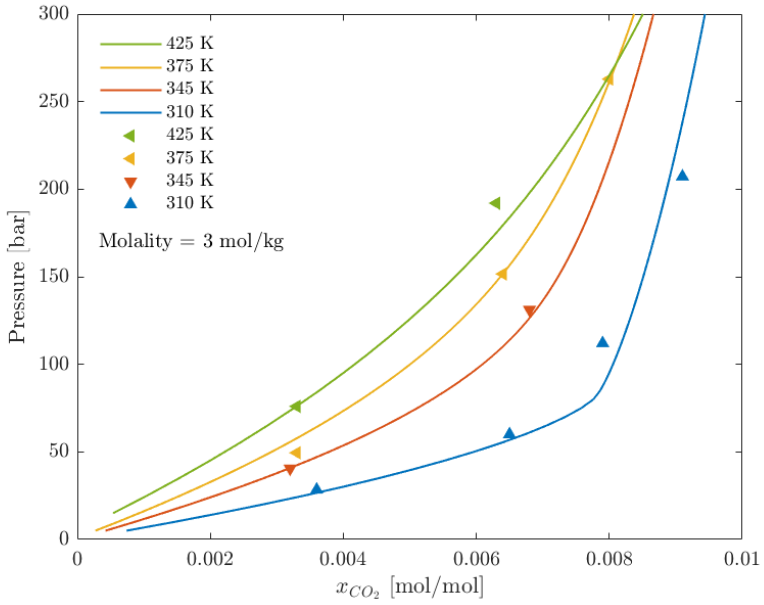

(c)

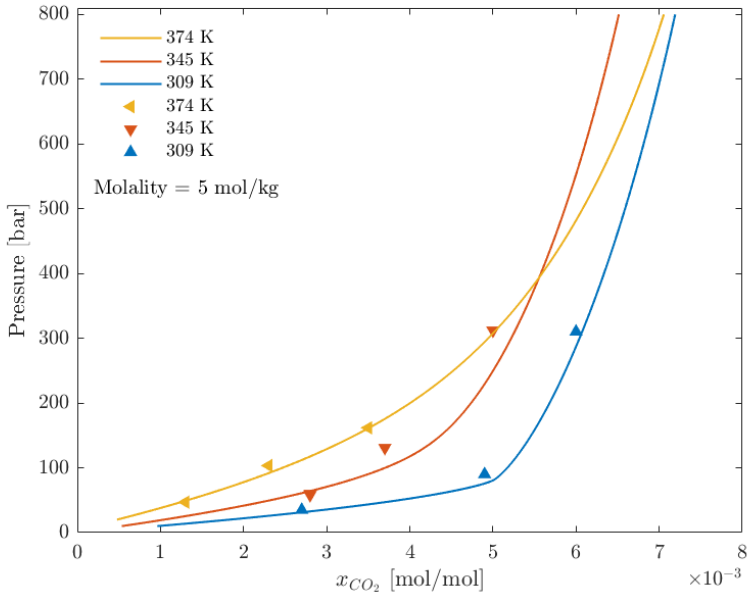

(d)

Figure 7. *p-x* diagram calculated for the CO_2+$MgCl_2$+H_2O system: (a) m=1.3 mol/kg; (b) m=2.31 mol/kg; (c) m=3 mol/kg; (d) m=5 mol/kg.

H_2O Fraction in the Gas Phase

The H_2O solubility in the gas phase can also be calculated by the model proposed in this work. **Figure 8** shows the comparison between the calculated and experimental H_2O contents in the non-aqueous phase for the CO_2+NaCl+H_2O system. The experimental data points are taken from Hou et al. (2013). As seen from **Figure 8a** and **Figure 8b**, over the temperature range of 323-423 K, the H_2O concentration calculated by Case 4 changes abruptly at pressures over 30 bar, which is caused by the transition from VLE to LLE. Similarly, the comparison between the calculated and measured H_2O concentration in the non-aqueous phase for the CO_2+KCl+H_2O system is shown in **Figure 9**, and the experimental data are also taken from Hou et al. (2013). In general, it can be seen that the developed thermodynamic model can well predict the concentration of H_2O in the non-aqueous phase with a satisfactory accuracy.

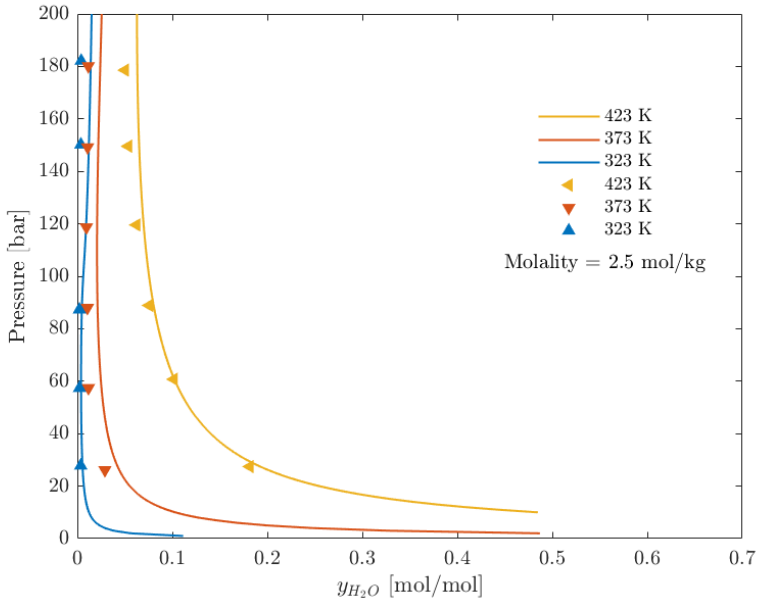

(a)

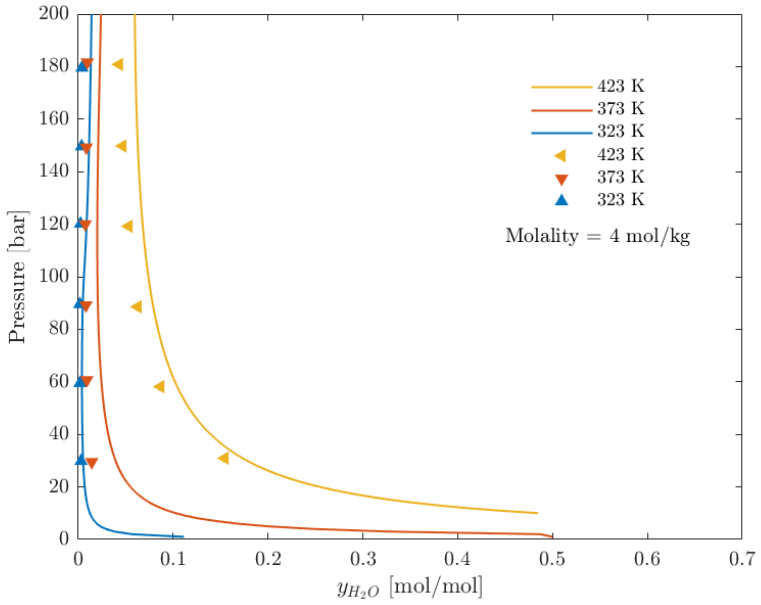

(b)

Figure 8. *p-y* diagram calculated for the CO_2+NaCl+H_2O system: (a) m=2.5 mol/kg; (b) m=4mol/kg.

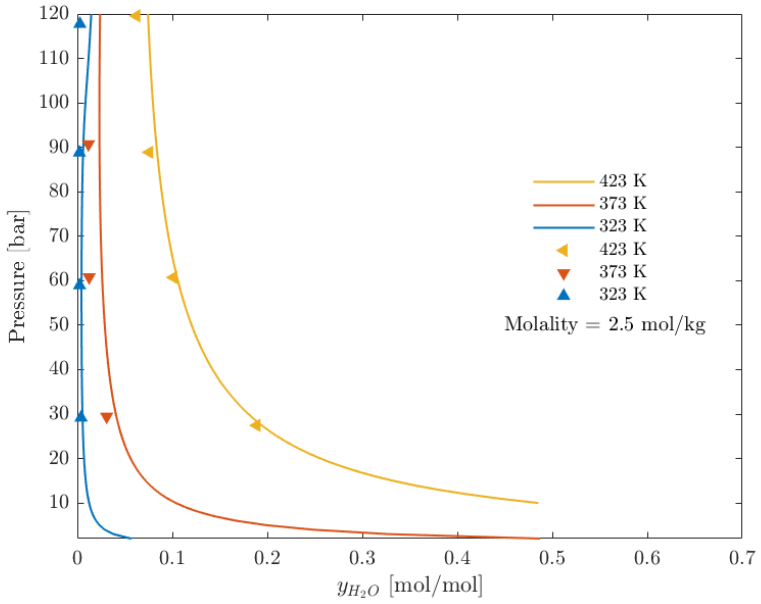

(a)

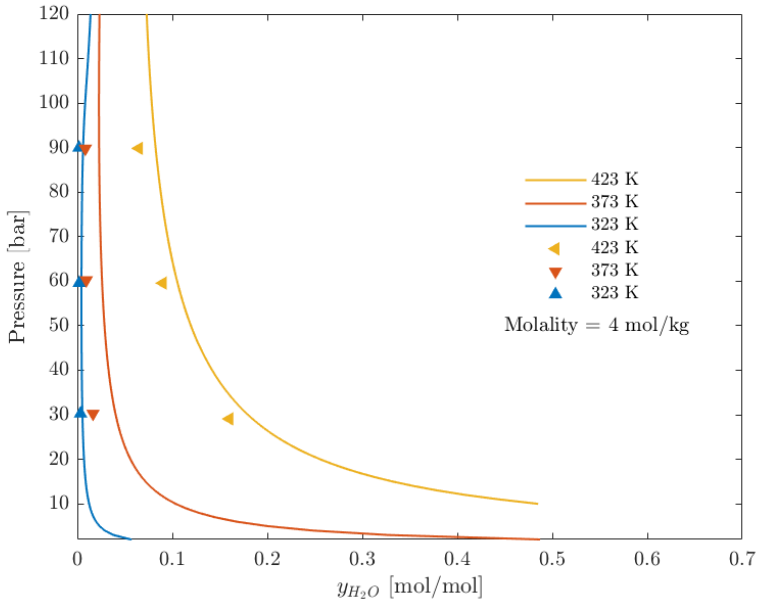

(b)

Figure 9. *p-y* diagram calculated for the CO_2+KCl+H_2O system: (a) m=2.5 mol/kg; (b) m=4 mol/kg.

Figure 10 compares the performance of the model proposed in this work against that of the Søreide & Whitson (1992) model for the CO_2+NaCl+H_2O systems. It also compares the performance of the model proposed in this work against that of the Sun et al. (2021) model for the four specific CO_2+single-salt+H_2O systems. As seen from **Figure 10**, the model proposed in this work gives better results than the two models in the literature in predicting the CO_2 solubility in the CO_2+single-salt+H_2O systems.

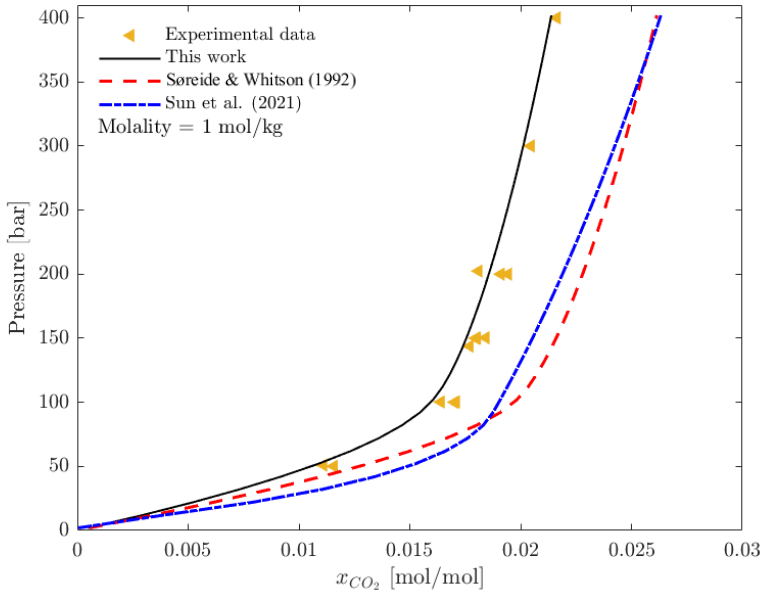
Experimental data
This work
Søreide & Whitson (1992)
Sun et al. (2021)
Molality = 1 mol/kg
Pressure [bar]
x_{CO_2} [mol/mol]
0
50
100
150
200
250
300
350
400
0.005
0.01
0.015
0.02
0.025
0.03

(a)

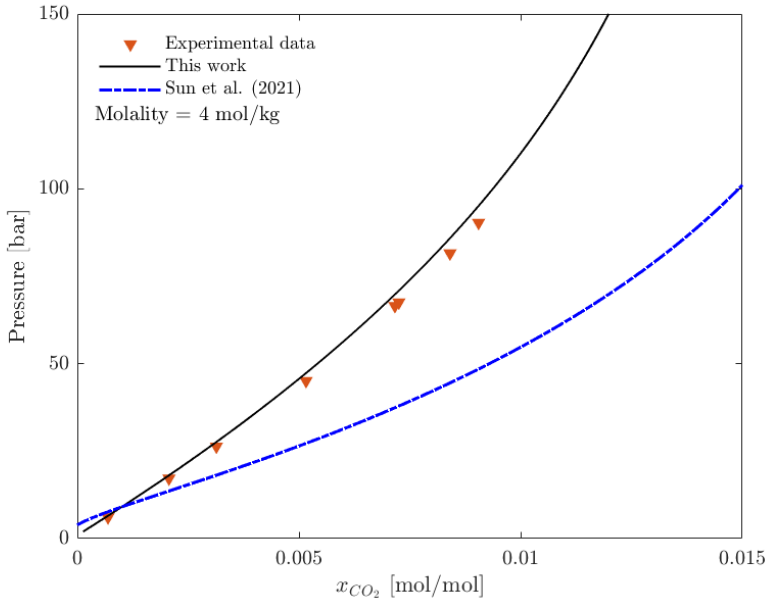
Experimental data
This work
Sun et al. (2021)
Molality = 4 mol/kg
Pressure [bar]
x_{CO_2} [mol/mol]
0
50
100
150
0.005
0.01
0.015

(b)

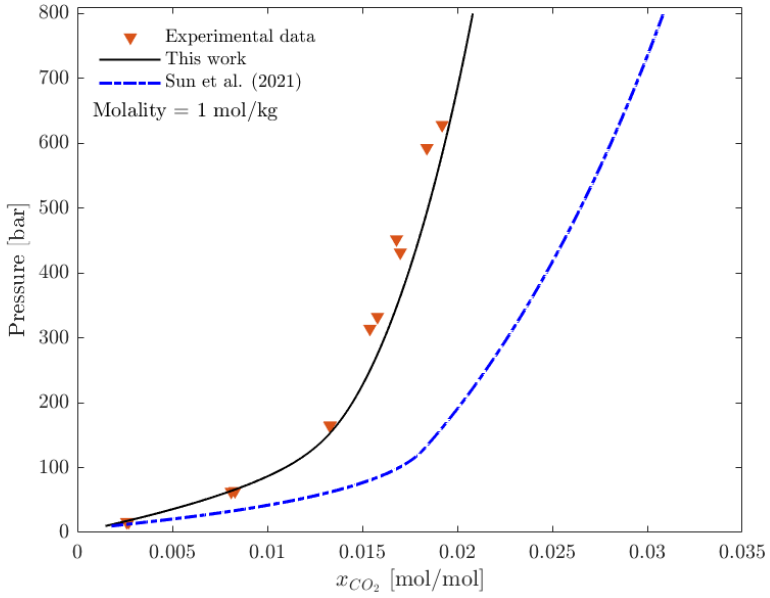

(c)

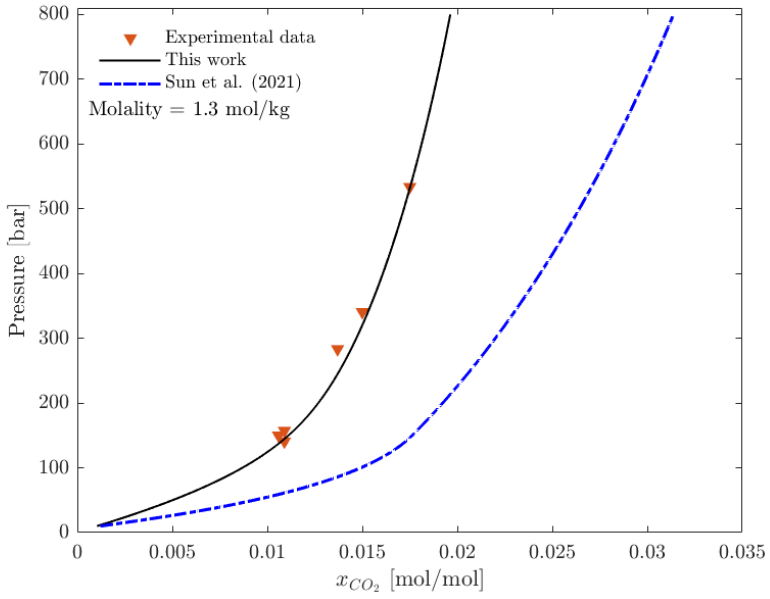

(d)

Figure 10. Calculated CO_2 solubility in the aqueous phase by different models versus the measured ones for the CO_2+single-salt+H_2O systems: (a) CO_2+NaCl+H_2O, T=323 K; (b) CO_2+KCl+H_2O, T=373 K; (c) CO_2+$CaCl_2$+H_2O, T=348 K; (d) CO_2+$MgCl_2$+H_2O, T=374 K.

Table 8 lists the detailed *%AAD* and *AAD* yielded by different models for the CO_2+single-salt+H_2O systems. As for the CO_2+NaCl+H_2O system, the model proposed in this work gives a

much higher accuracy in reproducing x_2 (i.e., 9.27*%AAD*) than the Søreide & Whitson (1992) model and the Sun et al. (2021) model. As for the other three systems (KCl, $CaCl_2$, and $MgCl_2$), the model proposed in this work also leads to a much higher accuracy (i.e., 6.10*%AAD*, 11.99*%AAD*, and 4.21*%AAD*).

Table 8. *%AAD* and *AAD* yielded by different models for the CO_2+NaCl+H_2O system.

Systems	Model	*%AAD*	*AAD*10³*
CO_2+NaCl+H_2O	Søreide & Whitson (1992)	32.61	1.96
	Sun et al. (2021)	57.99	6.59
	This work (Case 4)	**9.27**	**0.94**
CO_2+KCl+H_2O	Sun et al. (2021)	93.21	2.53
	This work (Case 4)	**6.10**	**0.48**
CO_2+$CaCl_2$+H_2O	Sun et al. (2021)	51.06	10.28
	This work (Case 4)	**11.99**	**0.97**
CO_2+$MgCl_2$+H_2O	Sun et al. (2021)	49.87	9.67
	This work (Case 4)	**4.21**	**0.37**

3.2.2 Model Performance for Mixed-Salt Brine Systems

Figure 11 compares the performance of the developed model against that of the Sun et al. (2021) model for mixed-salt brine systems over *T-P-M* ranges of 308-423 K, 10-600 bar, and 2.68-6.59 mol/kg. As seen from **Figure 11**, compared with the Sun et al. (2021) model, the model proposed in this work can more accurately predict the concentration of CO_2 in mixed-salt brines. Our model yields 12.63*%AAD* and 0.00146*AAD*, while the Sun et al. (2021) model yields 30.29*%AAD* and 0.0056*AAD*. The detailed comparison can be found in **Table 9.**

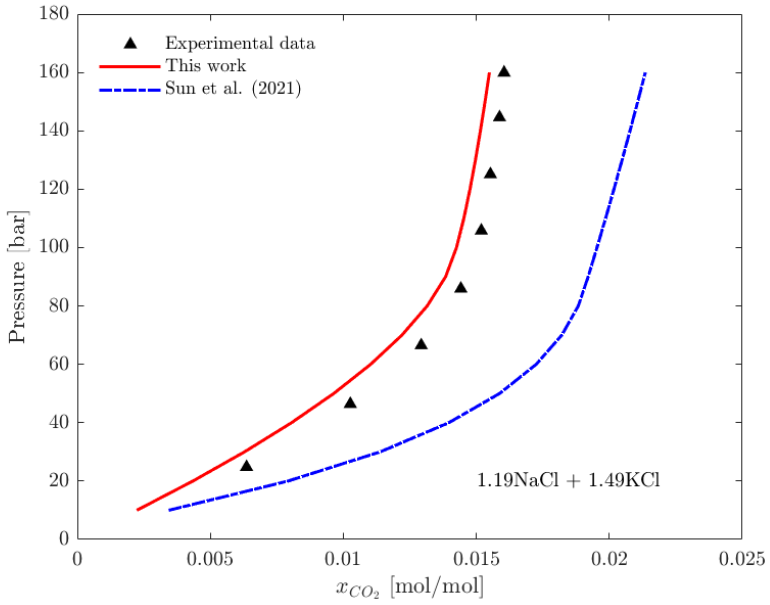
Experimental data
This work
Sun et al. (2021)
1.19NaCl + 1.49KCl
Pressure [bar]
x_{CO_2} [mol/mol]
0
20
40
60
80
100
120
140
160
180
0
0.005
0.01
0.015
0.02
0.025

(a)

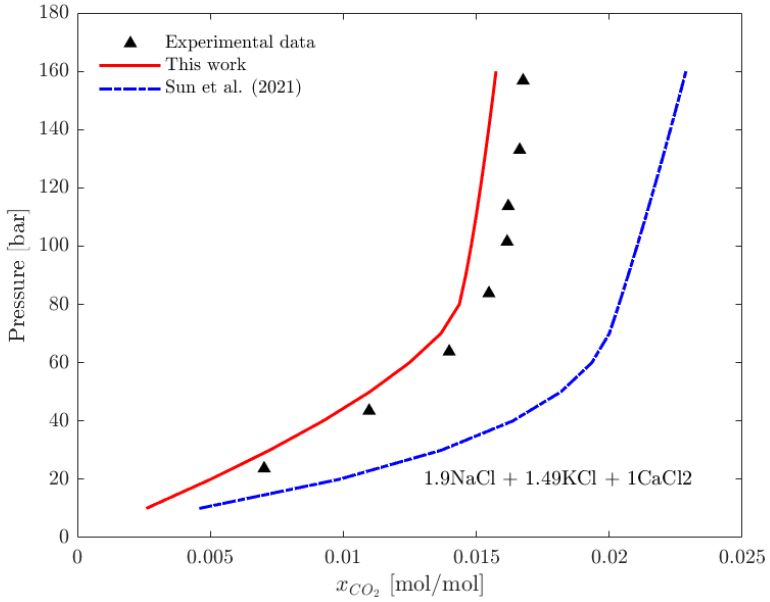
Experimental data
This work
Sun et al. (2021)
1.9NaCl + 1.49KCl + 1CaCl2
Pressure [bar]
x_{CO_2} [mol/mol]
0
20
40
60
80
100
120
140
160
180
0
0.005
0.01
0.015
0.02
0.025

(b)

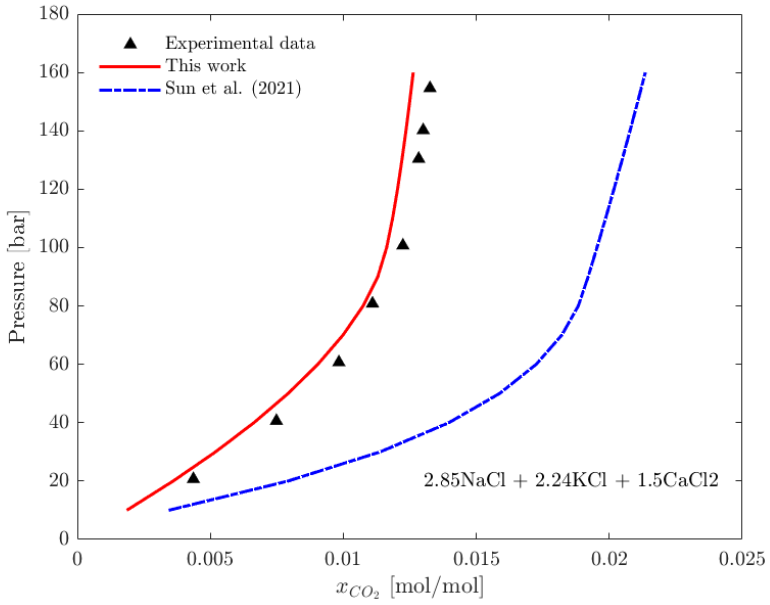
Experimental data
This work
Sun et al. (2021)
2.85NaCl + 2.24KCl + 1.5CaCl2
Pressure [bar]
x_{CO_2} [mol/mol]
0
20
40
60
80
100
120
140
160
180
0
0.005
0.01
0.015
0.02
0.025

(c)

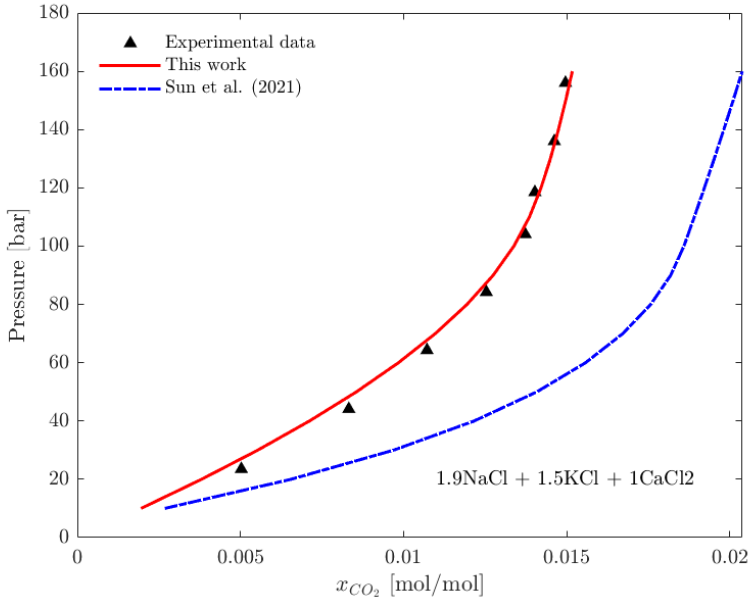
Experimental data
This work
Sun et al. (2021)
1.9NaCl + 1.5KCl + 1CaCl2
Pressure [bar]
x_{CO_2} [mol/mol]
0
20
40
60
80
100
120
140
160
180
0
0.005
0.01
0.015
0.02

(d)

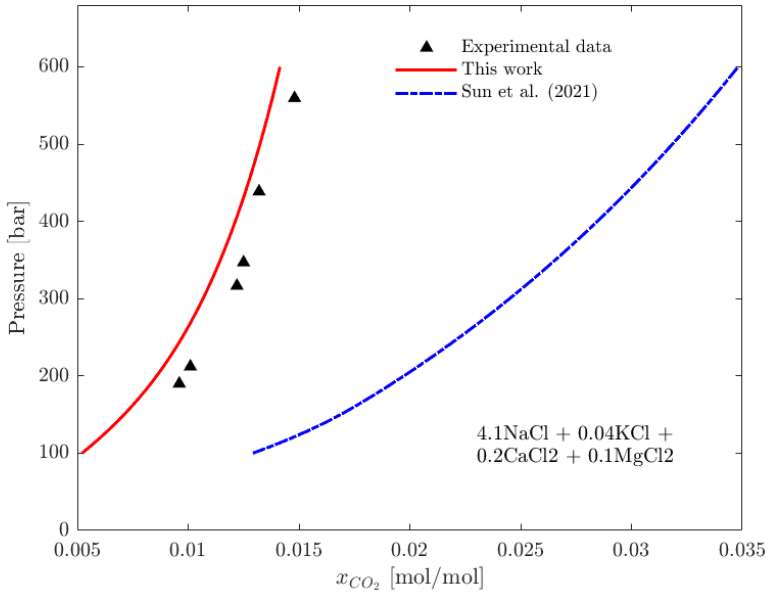

(e)

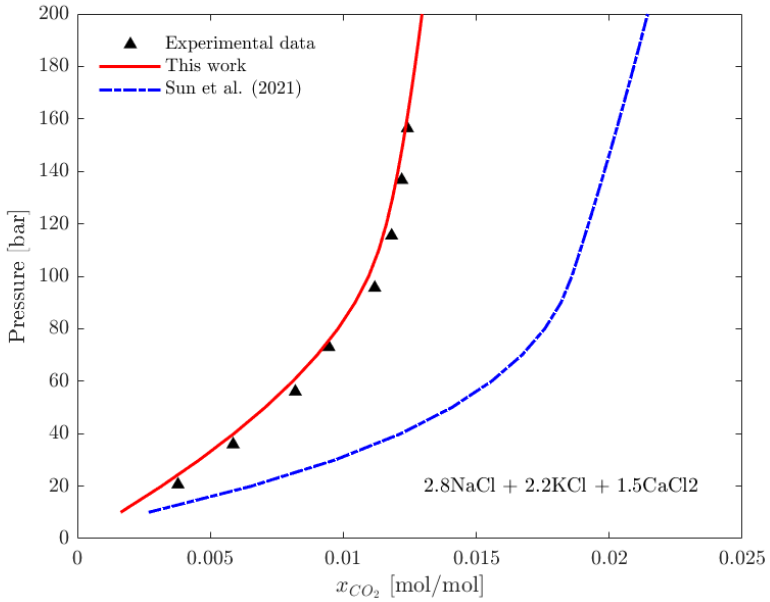

(f)

Figure 11. *p-x* diagram calculated for the CO_2+mixed-salt+H_2O systems: (a) T=318 K; (b) T=308 K; (c) T=318 K; (d) T=328 K; (e) T=423 K; (f) T=328 K.

Table 9. *%AAD* and *AAD* yielded by using different models for the CO_2+mixed-salt+H_2O system.

System	Model	*%AAD*	$AAD*10^3$
CO_2+Mixed-Salt+H_2O	Sun et al. (2021)	30.29	5.56
	This work	**12.63**	**1.46**

3.3 Impact of Salt Concentration on CO_2's Concentration in Water

Here we use the developed models to demonstrate the effect of salt concentration on CO_2 solubility. **Figure 12** shows the two solubility curves calculated at T=318 K for such purpose: one corresponds to CO_2 solubility in pure water, while the other corresponds to CO_2 solubility in a salty water. It can be clearly seen from **Figure 12** that, at 250 bar, the solubility of CO_2 in pure water is 2.75%, while it reduces to 1.66% when the total salt molality in the brine solution increases to 2.68 mol/kg. This means that the solubility of CO_2 in water is reduced by 40%, which significantly reduces the amount of CO_2 that can be stored in water. It can be concluded from the above discussion that the solubility trapping mechanism can be negatively affected by a higher salt concentration, and we would have to consider the impact of salt species and salt concentrations on the solubility trapping mechanism when we consider storing CO_2 in saline aquifers or depleted oil reservoirs.

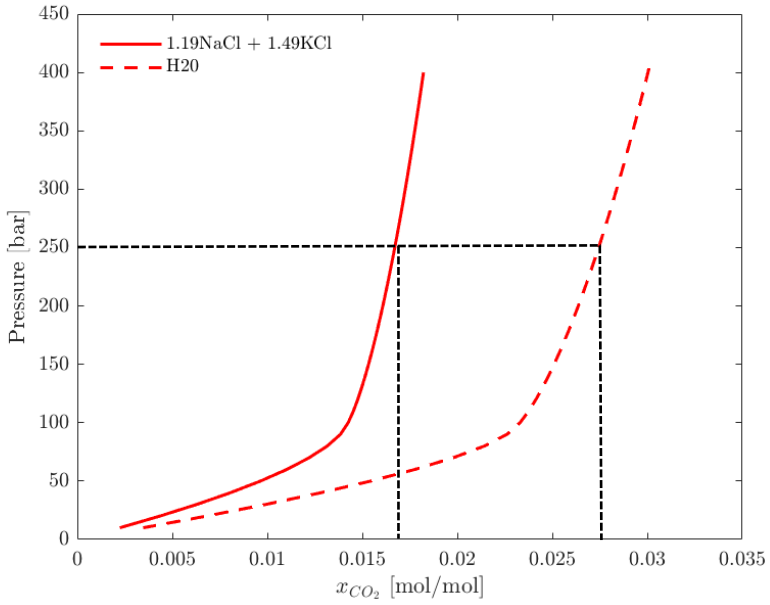

Figure 12. Comparison of *p*-*x* diagram for CO_2+H_2O system and CO_2+mixed-salt+H_2O system (*T*=318 K).

References

Abudour, A.M., Mohammad, S.A., & Gasem, K.A.M. (2012). Modeling high-pressure phase equilibria of coalbed gases/water mixtures with the Peng-Robinson equation of state. *Fluid Phase Equilibria*, 319, 77-89.

Hou, S.X., Maitland, G.C., & Trusler, J.P.M. (2013). Phase equilibria of (CO_2+H_2O+NaCl) and (CO_2+H_2O+KCl): Measurements and modeling. *Journal of Supercritical Fluids*,78, 78-88.

Søreide, I., & Whitson, C.H. (1992). Peng-Robinson predictions for hydrocarbons, CO_2, N_2, and H_2S with pure water and NaCl brine. *Fluid Phase Equilibria*, 77, 217-240.

Sun, X., Wang, Z., Li, H., He, H., & Sun, B. (2021). A simple model for the prediction of mutual solubility in CO_2-brine system at geological conditions. *Desalination*, 504(114972).

Yin, S., Wang, Z., Lu, C., & Li, H. (2020). Towards accurate phase behavior modeling for hydrogen sulfide/water mixtures. *Fluid Phase Equilibria*, 521, 112691.

CHAPTER 4 CONCLUSIONS AND RECOMMENDATIONS

4.1 Conclusions

In this work, a thermodynamic model is developed to better describe the phase behavior of CO_2+single-salt+H_2O systems and CO_2+mixed-salt+H_2O systems in the temperature range of 273-598 K, pressure range of 0.3-874 bar, and molality range of 0.017-6.59 mol/kg. Four commonly seen salts are considered: NaCl, KCl, $CaCl_2$, and $MgCl_2$. The major constituents of the thermodynamic model are PR EOS and Huron-Vidal mixing rule. The database used for optimizing the BIPs in the thermodynamic model includes experimental VLE and LLE data dedicated to CO_2+single-salt+H_2O systems and CO_2+mixed-salt+H_2O systems. The following conclusions can be made based on the research conducted in this study:

- The BIP, *k* value, in the Huron-Vidal mixing rule is dependent on temperature and salt molality. Moreover, the types of salt species also alter the optimal *k* values.
- The developed model can well capture the phase behavior of the four examined CO_2+single-salt+H_2O systems (NaCl, KCl, $CaCl_2$, and $MgCl_2$), among which the model yields the lowest error for $MgCl_2$ brines, while the model yields the highest error for $CaCl_2$ brines.
- The developed model outperforms the Søreide & Whitson (1992) model and the Sun et al. (2021) model for the CO_2+NaCl+H_2O system.
- The developed model outperforms the Sun et al. (2021) model for the CO_2+single-salt+H_2O systems.
- The thermodynamic model developed for the CO_2+mixed-salt+H_2O systems demonstrates a good performance in predicting the concentration of CO_2 in the CO_2+mixed-salt+H_2O systems and outperforms the Sun et al. (2021) model.

- The solubility trapping mechanism can be negatively affected by the presence of salt species and a higher salt concentration. When considering storing CO_2 in saline aquifers or depleted oil reservoirs, the impact of salt species and salt concentrations on the solubility trapping mechanism has to be taken into account.
- Since the key parameters in the thermodynamic model are determined based on the experimental data available in the literature, one should be cautious when using the developed model to predict CO_2 solubility in brines at conditions that are different from the ones covered by the literature data.

4.2 Recommendations

Reliable experimental phase equilibrium data of CO_2/brine mixtures should be made available in the future to examine the model performance at elevated pressures, temperatures, and low molality (p>400 bar, T> 523 K, and M<1 mol/kg). Among the systems discussed in this study, we are currently in need of more experimental data of CO_2 solubility in CO_2+KCl+H_2O, CO_2+$CaCl_2$+H_2O, CO_2+$MgCl_2$+H_2O, and CO_2+mixed-salt+H_2O systems. In addition, different alpha-functions in PR EOS can influence the predictive capability of EOS to a large degree. It is desirable to further explore the use of more appropriate alpha functions in PR EOS such that the enhanced PR EOS model can become capable of more accurately predicting the VLE/LLE equilibria CO_2/brine mixtures at high temperatures (T>523 K) and high pressures (p>400 bar).

References

Søreide, I., & Whitson, C.H. (1992). Peng-Robinson predictions for hydrocarbons, CO_2, N_2, and H_2S with pure water and NaCl brine. *Fluid Phase Equilibria*, 77, 217-240.

Sun, X., Wang, Z., Li, H., He, H., & Sun, B. (2021). A simple model for the prediction of mutual solubility in CO_2-brine system at geological conditions. *Desalination*, 504, 114972.

BIBLIOGRAPHY

Abba, M.K., Abbas, A.J., Nasr, G.G., Al-Otaibi, A., Burby, M., Saidu, B., & Suleiman, S.M. (2019). Solubility trapping as a potential secondary mechanism for CO_2 sequestration during enhanced gas recovery by CO_2 injection in conventional natural gas reservoirs: an experimental approach. *Journal of Natural Gas Science and Engineering*, 71, 103002.

Abudour, A.M., Mohammad, S.A., & Gasem, K.A.M. (2012). Modeling high-pressure phase equilibria of coalbed gases/water mixtures with the Peng-Robinson equation of state. *Fluid Phase Equilibria*, 319, 77-89.

Anderko, A., & Pitzer, K.S. (1993). Equation-of-state representation of phase equilibria and volumetric properties of the system NaCl-H_2O above 573 K. *Geochimica Et Cosmochimica Acta*, 57(8), 1657-1680.

Bachu, S., Bonijoly, D., Bradshaw, J., Burruss, R., Holloway, S., Christensen, N.P., & Mathiassen, O.M. (2007). CO_2 storage capacity estimation: Methodology and gaps. *International Journal of Greenhouse Gas Control*, 1(4), 430-443.

Bando, S., Takemura, F., Nishio, M., Hihara, E., & Akai, M. (2003). Solubility of CO_2 in aqueous solutions of NaCl at (30 to 60)°C and (10 to 20) MPa. *Journal of Chemical and Engineering Data*, 48(3), 576-579.

Bastami, A., Allahgholi, M., & Pourafshary, P. (2014). Experimental and modelling study of the solubility of CO_2 in various $CaCl_2$ solutions at different temperatures and pressures. *Petroleum Science*, 11(4), 569-577.

Bermejo, M.D., Martín, A., Florusse, L.J., Peters, C.J., & Cocero, M.J. (2005). The influence of Na_2SO_4 on the CO2 solubility in water at high pressure. *Fluid Phase Equilibria*, 238(2), 220-228.

Chabab, S., Théveneau, P., Corvisier, J., Coquelet, C., Paricaud, P., Houriez, C., & Ahmar, E.El. (2019). Thermodynamic study of the CO_2-H_2O-NaCl system: Measurements of CO_2 solubility and modeling of phase equilibria using Soreide and Whitson, electrolyte CPA and SIT models. *International Journal of Greenhouse Gas Control*, 91, 102825.

Chamwudhiprecha, N., & Blunt, M.J. (2011). CO_2 storage potential in the North Sea. *In International Petroleum Technology Conference*. *OnePetro*.

Diamond, L.W., & Akinfie, N.N. (2003). Solubility of CO_2 in water from -1.5 to 100°C and from 0.1 to 100 MPa: Evaluation of literature data and thermodynamic modelling. *Fluid Phase Equilibria*, 208(1-2), 265-290.

Ding, S., Xi, Y., Jiang, H., Liu, G. (2018). CO_2 storage capacity estimation in oil reservoirs by solubility and mineral trapping. *Applied Geochemistry*, 89, 121-128.

Duan, Z., Møller, N., & Weare, J.H. (1992). An equation of state for the CH_4-CO_2-H_2O system: II. Mixtures from 50 to 1000 °C and 0 to 1000 bar. *Geochimica et Cosmochimica Acta*, 56(7), 2619-2631.

Duan, Z., & Sun, R. (2003). An improved model calculating CO_2 solubility in pure water and aqueous NaCl solutions from 273 to 533 K and from 0 to 2000 bar. *Chemical Geology*, 1(1-2), 257-271.

Ellis, A.J., & Golding, R.M. (1963). The solubility of carbon dioxide above 100 degrees C in water and in sodium chloride solutions. *American Journal of Science*, 261(1), 47-60.

Gilbert, K., Bennett, P.C., Wolfe, W., Zhang, T., & Romanak, K.D. (2016). CO_2 solubility in aqueous solutions containing Na^+, Ca_2^+, Cl^-, SO_4^{2-} and HCO_3^-: The effects of electrostricted water and ion hydration thermodynamics. *Applied Geochemistry*, 67, 59-67.

Guo, H., Huang, Y., Chen, Y., & Zhou, Q. (2016). Quantitative Raman spectroscopic measurements of CO_2 solubility in NaCl solution from (273.15 to 473.15) K at P = (10.0, 20.0, 30.0, and 40.0) MPa. *Journal of Chemical and Engineering Data*, 61(1), 466-474.

Haas, J.L. (1976). Physical properties of the coexisting phases and thermochemical properties of the H_2O component in boiling NaCl solutions. *Geological Survey Bulletin*, 1421-A.

He, S., & Morse, J.W. (1993). The carbonic acid system and calcite solubility in aqueous Na-K-Ca-Mg-Cl-SO_4 solutions from 0 to 90°C. *Geochimica Et Cosmochimica Acta*, 57(15), 3533-3554.

Hou, S.X., Maitland, G.C., & Trusler, J.P.M. (2013). Phase equilibria of (CO_2+H_2O+NaCl) and (CO_2+H_2O+KCl): Measurements and modeling. *Journal of Supercritical Fluids*, 78, 78-88.

Huron, M.J., & Vidal, J. (1979). New mixing rules in simple equations of state for representing vapor-liquid equilibria of strongly non-ideal mixtures. *Fluid Phase Equilibria*, 3, 255-271.

Jacob, R., & Saylor, B.Z. (2016). CO_2 solubility in multi-component brines containing NaCl, KCl, $CaCl_2$ and $MgCl_2$ at 297 K and 1-14 MPa. *Chemical Geology*, 424, 86-95.

Kamps, Á.P.S., Meyer, E., Rumpf, B., & Maurer, G. (2007). Solubility of CO_2 in aqueous solutions of KCl and in aqueous solutions of K_2CO_3. *Journal of Chemical and Engineering Data*, 52(3), 817-832.

Kiepe, J., Horstmann, S., Fischer, K., & Gmehling, J. (2002). Experimental determination and prediction of gas solubility data for CO_2+H_2O mixtures containing NaCl or KCl at temperatures between 313 and 393 K and pressures up to 10 MPa. *Industrial & Engineering Chemistry Research*, 41(17), 4393-4398.

Koschel, D., Coxam, J.Y., Rodier, L., & Majer, V. (2006). Enthalpy and solubility data of CO_2 in water and NaCl(aq) at conditions of interest for geological sequestration. *Fluid Phase Equilibria*, 247(1-2), 107-120.

Lindeloff, N., & Michelsen, M. (2003). Phase envelope calculations for hydrocarbon-water mixtures. *SPE Journal,* 8(3), 298-303.

Liu, Y., Hou, M., Yang, G., & Han, B. (2011). Solubility of CO_2 in aqueous solutions of NaCl, KCl, $CaCl_2$ and their mixed salts at different temperatures and pressures. *Journal of Supercritical Fluids*, 56(2), 125-129.

Messabeb, H., Contamine, F., Cézac, P., Serin, J.P., & Gaucher, E.C. (2016). Experimental measurement of CO_2 solubility in aqueous NaCl solution at temperature from 323.15 to 423.15 K and pressure of up to 20 MPa. *Journal of Chemical and Engineering Data*, 61(10), 3573-3584.

Michelsen, M.L. (1982) The isothermal flash problem. Part I. Stability. *Fluid Phase Equilibria*, 9, 1-19.

Mohammadian, E., Hamidi, H., Asadullah, M., Azdarpour, A., Motamedi, S., & Junin, R. (2015). Measurement of CO_2 solubility in NaCl brine solutions at different temperatures and pressures using the potentiometric titration method. *Journal of Chemical and Engineering Data*, 60(7), 2042-2049.

Nighswander, J.A., Kalogerakis, N., & Mehrotra, A.K. (1989). Solubilities of carbon dioxide in water and 1 wt. % NaCl solution at pressures up to 10 MPa and temperatures from 80 to 200 °C. *Journal of Chemical and Engineering Data*, 34(3), 355-360.

Peng, D., & Robinson, D.B. (1976). A new two-constant equation of state. *Industrial & Engineering Chemistry Research*, 15(1), 59-64.

Poulain, M., Messabeb, H., Lach, A., Contamine, F., Cézac, P., Serin, J.P., Dupin, J.C., & Martinez, H. (2019). Experimental measurements of carbon dioxide solubility in Na-Ca-K-Cl solutions at high temperatures and pressures up to 20 MPa. *Journal of Chemical and Engineering Data*, 64(6), 2497-2503.

Prutton, C., & Savage, R. (1940). The solubility of carbon dioxide in calcium chloride-water solutions at 75, 100, 120°C and high pressures. *Journal of the American Chemical Society*, 67(9), 1550-1554.

Rachford Jr, H.H. & Rice, J.D. (1952). Procedure for use of electronic digital computers in calculating flash vaporization hydrocarbon equilibrium. *Journal of Petroleum Technology*, 410, 19-3.

Renon, H., & Prausnitz, J.M. (1968). Local compositions in thermodynamic excess functions for liquid mixtures. *AIChE Journal*, 14(1), 135-144.

Rumpf, B., Nicolaisen, H., Öcal, C., & Maurer, G. (1994). Solubility of carbon dioxide in aqueous solutions of sodium chloride: Experimental results and correlation. *Journal of Solution Chemistry,* 23(3), 431-448.

Savary, V., Berger, G., Dubois, M., Lacharpagne, J.C., Pages, A., Thibeau, S., & Lescanne, M. (2012). The solubility of CO_2+H_2S mixtures in water and 2M NaCl at 120°C and pressures up to 35 MPa. *International Journal of Greenhouse Gas Control*, 10, 123-133.

Sminchak, J.R., Babarinde, O., & Gupta, N. (2017). Integrated analysis of geomechanical factors for geologic CO_2 Storage in the midwestern United States. *Energy Procedia*,114, 3267-3272.

Soave, G. (1972). Equilibrium constants from a modified Redlich-Kwong equation of state. *Chemical Engineering Science*, 27(6), 1197-1203.

Søreide, I., & Whitson, C.H. (1992). Peng-Robinson predictions for hydrocarbons, CO_2, N_2, and H_2S with pure water and NaCl brine. *Fluid Phase Equilibria*, 77, 217-240.

Sørensen, H., Pedersen, K.S., & Christensen, P.L. (2002). Modeling of gas solubility in brine. *Organic Geochemistry*, 33(6), 635-642.

Springer, R.D., Wang, Z., Anderko, A., Wang, P., & Felmy, A.R. (2012). A thermodynamic model for predicting mineral reactivity in supercritical carbon dioxide: I. Phase behavior of carbon dioxide-water-chloride salt systems across the H_2O-rich to the CO_2-rich regions. *Chemical Geology*, 322-323, 151-171.

Sun, X., Wang, Z., Li, H., He, H., & Sun, B. (2021). A simple model for the prediction of mutual solubility in CO_2-brine system at geological conditions. *Desalination*, 504, 114972.

Teymouri, S. (2016). Phase equilibria measurements and modelling of CO_2-rich fluids/brine systems. PhD Dissertation. Heriot-Watt University.

Trusler, J.P.M. (2017). Thermophysical properties and phase behavior of fluids for application in carbon capture and storage processes. Annual Review of Chemical and Biomolecular Engineering, 8(1), 381402.

Tong, D., Trusler, J.P.M., & Vega-Maza, D. (2013). Solubility of CO2 in aqueous solutions of $CaCl_2$ or $MgCl_2$ and in a synthetic formation brine at temperatures up to 423 K and pressures up to 40 MPa. *Journal of Chemical and Engineering Data*, 58(7), 2116-2124.

Whitson, C.H., & Brulé, M.R. (2000). Phase behavior. SPE Monograph.

Wilson, G.M. (1969). Modified Redlich-Kwong equation of state, application to general physical data calculations. *65th National AIChE Meeting*, Cleveland, OH, 15.

Wong, D.S.H., & Sandler, S.I. (1992). A theoretically correct mixing rule for cubic equations of state. *AIChE Journal*, 38(5), 671-680.

Xiao, T., McPherson, B., Pan, F., Esser, R., Jia, W., Bordelon, A., & Bacon, D. (2016). Potential chemical impacts of CO_2 leakage on underground source of drinking water assessed by quantitative risk analysis. *International Journal of Greenhouse Gas Control*, 50, 305-316.

Yan, W., Huang, S., & Stenby, E.H. (2011). Measurement and modeling of CO_2 solubility in NaCl brine and CO_2-saturated NaCl brine density. *International Journal of Greenhouse Gas Control*, 5(6), 1460-1477.

Yin, S., Wang, Z., Lu, C., & Li, H. (2020). Towards accurate phase behavior modeling for hydrogen sulfide/water mixtures. *Fluid Phase Equilibria*, 521, 112691.

Zhao, H., Dilmore, R.M., & Lvov, S.N. (2015). Experimental studies and modeling of CO_2 solubility in high temperature aqueous $CaCl_2$, $MgCl_2$, Na_2SO_4, and KCl solutions. *AIChE Journal*, 61(7), 2286-2297.

Zhao, H., Fedkin, M.V., Dilmore, R.M., & Lvov, S.N. (2015). Carbon dioxide solubility in aqueous solutions of sodium chloride at geological conditions: Experimental results at 323.15, 373.15, and 423.15K and 150 bar and modeling up to 573.15 K and 2000 bar. *Geochimica Eet Cosmochimica Acta*, 149, 165-189.

Zhao, H., & Lvov, S.N. (2016). Phase behavior of the CO_2-H_2O system at temperatures of 273-623 K and pressures of 0.1-200 MPa using Peng-Robinson-Stryjek-Vera equation of state with a modified Wong-Sandler mixing rule: an extension to the CO_2-CH_4-H_2O system. *Fluid Phase Equilibria*, 417, 96-108.